DELIVERABLE 3.3.4

FP7-ENERGY-2008-TREN-1

Grant Agreement No: **239349**

ACRONYM: **H2-IGCC**

Preliminary Turbine Cooling Requirement

ROMA TRE UNIVERSITÀ DEGLI STUDI Mechanical and Industrial Engineering Department

RO3 Scientific Responsible: **Prof. Giovanni Cerri**

Collaborators:

F. Botta, L. Chennaoui, A. Giovannelli, C. Salvini, C. Basilicata, S. Mazzoni, E. Archilei

DISSEMINATION LEVEL: PUBLIC Date of issue 01-08-2013

Deliverable 3.3.4

Preliminary Turbine Cooling Requirement

Please send your feedback to G. Cerri, Organisation: RO3, cerri@uniroma3.it

DISSEMINATION LEVEL: PUBLIC

Index

Index of figures

Nomenclature

BAT	Best Available Technology
BM	Bulk Material
c_p	specific heat capacity
CC	Combustion Chamber
CFD	Computational Fluid Dynamics
CTCR	Coolant Thermal Capacity Rate
DB	*Data Base*
Eff	Effectiveness
FOB	Objective Function
FV	Finite Volume
GT	Gas Turbine
U_J	Heat Transfer Coefficient of j-th flow
HDGT	Heavy Duty Gas Turbine
HGTCR	Hot Gas Thermal Capacity Rate
IGCC	Integrated Gasification Combined Cycle
LHV	Low Heating Value
LP	Lumped Performance
m	Mass Flow
n	Shaft Rotational Speed rpm
N	Index
NTU	Number of Heat Transfer Units
p	Pressure
P	Power
PR	Pressure Ratio
RH	Relative Humidity
Q	Heat
s	Thickness
S	Surface
SoA	State of the Art
T	Temperature
Tc	Coolant temperature
Tf	Firing Temperature
Tg	Hot gas temperature
Tw	Blade wall temperature
TBC	Thermal Barrier Coating
TIT	Turbine Inlet Temperature
TCR	Thermal Capacity Ratio
U	Global Heat Transfer Coefficient
UEBC	Uncooled Equivalent Brayton Cycle
VIGV	Variable Inlet Guide Vanes

Greek Symbols

β	Pressure Ratio
λ	Thermal Conductivity
μc	Thermal Capacity Ratio
ε	Heat Transfer Effectiveness
η_c	Cooling Effectiveness
ρ	Density

Subscripts

0	Reference Condition / Standard Condition
b	Blade
b_J	j-th bleed
c	Coolant
C	Compressor
E	Expander
ex	Exhaust Gas
g	Gas
i	Inlet
N	Nominal
o	Outlet
R_J	j-th rotor
S_J	j-th stator

1 Introduction

Modern Heavy Duty and Aero Gas Turbine engines are the most complex system being operated because many interconnected phenomena assure the maximum exploitation on the sophisticated high performance material based devices (e.g. vanes, blades, shrouds, seals, etc.) for a sufficient operation time at temperatures that assure economic revenue of the money investments.

Gas Turbine engine performance work (work for kg of the air entering the compressor – power for kg/s of the air entering the compressor) and efficiency (i.e. heat consumption for an unit of produced work, heat rate for an unit or delivered power) depend on the flow-weighted mean temperature of the working fluid entering the expander (TIT), on the exhaust temperature that is related to the TIT, on the pressure ratio of the expander, on the fuel composition and of its low heating value , on the entropy production (or dissipated work), on the boundary conditions (ambient, speed, etc.) and on the heat removed from the expander along the flow path.

Of course temperature levels are related to the component life consumption rate due to operation that involves also stress, corrosion, erosion and other facts that are summarized under the creep concept.

To rise firing temperatures maintaining the temperatures of the GT hot components lower than the threshold allowed by the material characteristic the cooling concept has been adopted. This means that some fresh cooling mean is introduced inside the expander disks, blades, etc. to remove the heat flowing from the outer main stream and to overall decrease the metal temperature. Under this context internal channels with enhancer heat transfer devices lead the coolant mass flow to imping some areas of the internal surface and escape to the lateral surface especially at the leading edge producing a film and at the trailing edge passing through slots made of finned surface.

In the H2-IGCC Project context RO3 has developed an Generic 300MW F Class Gas Turbine Simulator that adopts a Lumped Performance (LP) methodology employing a Finite Volume (FV) approach based on detailed Architecture, Geometry, Lumped Physics and Chemistry including all the empirically known phenomena characterizing the specific Gas Turbine behaviour. Such a simulator has been built up taking the Best Available Technologies (BAT) connected to the existing F, G and H Class Gas Turbines of many Manufacturers into account. Features of such a simulator have been developed as to be close to those of the existing machines of some European O&M's.

The main quantities characterizing the GT (Firing Temperature, Turbine Inlet Temperature, Turbine Exhaust Temperature, Exhaust Mass Flow, Pressure Ratio, Power, Overall Efficiency, etc.) has been taken during the Generic 300MW F Class GT Simulator development into consideration, looking at the BAT and to the selected architecture of the

Generic 300MW F Class GT that has been chosen to that of the Ansaldo AE 94.3A and Siemens SGT5-4000F ones, the manufacturer being partners of the project.

In this deliverable, the preliminary evaluation of the overall cooling mass flow is discussed. To perform this calculation after a preliminary cycle calculation, in which GT global quantities such as temperatures, mass flows, etc. have been evaluated, the overall coolant mass flow has been established by the adoption of global models according to the BAT State of the Art (SoA) and Technological Background.

Once the overall coolant mass flow has been evaluated, cooling requirement for each expander row has been calculated taking the RO3 lumped model approach into account.

Coolant mass flows required to cool the Generic 300MW F Class Gas Turbine fed by Methane at the nominal running point are reported. Such a calculation has been also performed for the 33 MJ/kg Syngas fed re-staggered Gas Turbine that is the pervious one with the 1st Nozzle Vane (NV) opened (re-staggered) to accommodate the increase of the turbine inlet mass flow connected with the reduction of the LHV.

2 Uncooled Cycle Calculation

A preliminary evaluation of a methane (CH4) fed GT cycle has been performed to evaluate the relevant quantities (temperature, pressure, etc.) in the GT main stations (compressor inlet and outlet, expander inlet and outlet, etc.) that allow to establish global parameters need to develop the Generic 300MW F Class GT Simulator, according to the present SoA.
In figure 1, the ideal ($12_s3'4'_s1$), the real (123'4'1) and the Uncooled Equivalent (12341) Brayton Cycles are represented:

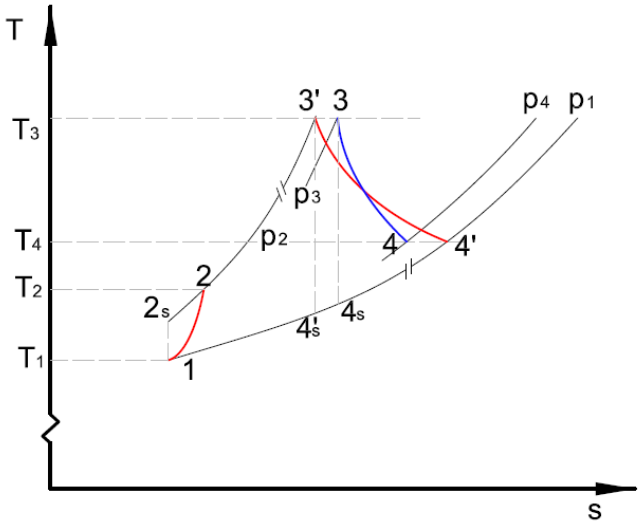

Fig. 1: Scheme of a GT Brayton Cycle – Not to Scale

The Uncooled Equivalent Brayton Cycle model developed by RO3 takes the various GT losses by the introduction of polytropic efficiencies (compressor, expander) as well as the combustion efficiency and by the introduction of the total pressure loss both in the combustion chamber and in the exhaust duct into consideration. Under this assumption the ideal cycle ($12_s3'4'_s1$) is stretched in the UEBC (12341). Schematically, the sketch of the GT well representing the UEBC is depicted in figure 2:

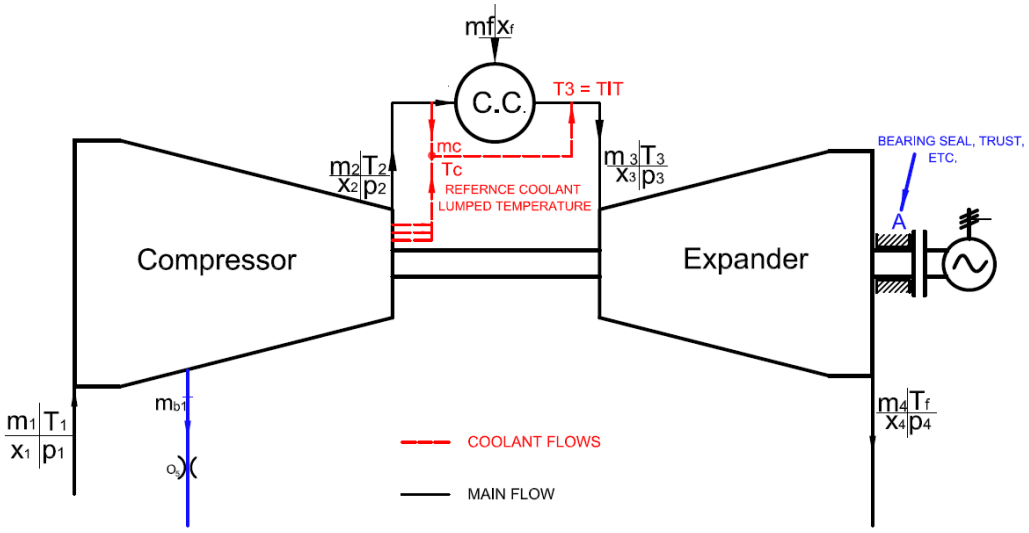

Fig. 2: Scheme of a Generic 300MW F Class GT

UEBC Calculation has been performed taking data of the present State of the art of the BAT GT. In table 1 some of these data are given:

Table 1: HD GTs Characteristic Quantities

	Power [MW]	Efficiency [%]	Exhaust Temp [°C]	Exhaust Mass [kg/s]	Pressure Ratio [#]
Siemens (2008) SGT5 - 4000F	292	39.8	577	692	18.2
Siemens (2013) SGT5 - 4000F	295	40.0	586	692	18.8
Ansaldo AE 94.3A	294	39.7	580	702	18.2
Mitsubishi (2012) M701F4	324	39.9	592	730	18
Alstom (2012) GT 26*	326	40.3	603	692	35

*: HDGT with a 'Sequential Combustion'

To perform the calculation, some parameters have been fixed to be varied into a feasible domain according with the BAT to evaluate the relevant quantities of the GT Cycle.

- ηc: compressor efficiency
- ηe: expander efficiency
- ηb: combustion efficiency (taking the unburned into account).

  The combustion efficiency does not take the not fully adiabaticity of the process into account. This aspect is considered instead when the combustor efficiency is introduced.
- Qsb: GT radiation and convection heat losses (some 1%)
- Δp: pressure loss (combustor and exhaust duct)
- P loss: Losses (mechanic loss and electric loss)

  All the mechanic loss (including the thrust) are schematically lumped in the section A of the figure 2. Electric loss includes both the transformer loss and the electric generator loss.

By the solution of a set of equations fully describing the Uncooled Equivalent Brayton Cycle, properly bounded by a set of inequalities, the quantities needed for the preliminary cooling calculation have been evaluated.

Inlet quantities and outlet quantities of the UEBC Calculation are given in tables 2 and 3:

Table 2: Input Data for Cycle Calculation

		AE 94.3A	SGT5-4000F
BOUNDARY CONDITIONS (**b**)			
p1	[kPa]	101.3	101.3
T1	[°C]	15.0	15.0
[xx]1	[#]m	dry air + RH60%	
DATA (**d**)			
[xx]f	[#]m	pure methane	
LHV	[kJ/kg]	50060	50060
P*	[MW]	294	292
ηGT*	[#]	0.397	0.397
mex*	[kg/s]	702	692
Tex*	[°C]	580	577
β*	[#]	18.2	18.2
Δpcc/p2	[#]	0.05	0.05
Δpe/p1	[#]	0.03	0.03
ηm	[#]	0.998	0.998
ηge	[#]	0.968	0.968

Table 3: Cycle Calculated Quantities

		AE 94.3A	SGT5 - 4000F
COMPRESSOR			
T1	[°C]	15	15
T2	[°C]	409	409
p2	[kPa]	1844.1	1844.1
etapc	[#]	0.929	0.928
LC	[kJ/kg]	411	411
COMBUSTION CHAMBER			
etacc	[#]	0.99	0.99
AFR	[#]	46	46
EXPANDER			
T3	[°C]	1246	1246
p3	[kPa]	1751.9	1751.9
etape	[#]	0.866	0.871
LE	[kJ/kg]	854	858
GAS TURBINE			
LTg	[kJ/kg]	428	431

Taking data of the Reference GT given in table 1 (i.e. exhaust mass flow) into account the compressor inlet mass flow and fuel mass can be established as well as power that have not been calculated by the Uncooled Equivalent Brayton Cycle calculation because it is a specific cycle calculation.

Table 4: Cycle Mass Flows

		AE 94.3A	SGT5 - 4000F
Mass Flow			
mCi	[kg/s]	687.2	677.3
mf	[kg/s]	14.8	14.7
mex	[kg/s]	702.0	1844.1

As a result of the UEBC evaluation , the expander inlet temperature T3 has been established. According with figures 1 and 2, in the UEBC the T3 is the Turbine Inlet Temperature (TIT) defined by the ISO 2314,where Turbine Inlet Temperature is defined:

'defined arbitrarily as a theoretical flow-weighted mean temperature before the first-stage stationary blades calculated from an overall heat balance of the combustion chamber with the gas mass flow from combustion mixed with the turbine cooling air mass flows prior to entering the first stage stationary blades'.

Accordingly, TIT can be approximated by the rule (1) according to figure 3:

$$TIT \approx \frac{m_g \cdot c_{pg} \cdot T_g + \sum_j m_{cj} \cdot c_{pj} \cdot T_{cj}}{m_{mix} \cdot c_{pmix}} \qquad (1)$$

m_{mix} being the sum of the various coolant flows m_{cj} and of the gas mass flow m_g and c_{pmix} being the pressure constant specific heat of the mixture depending on many parameters.

$$c_{pmix} = f[c_{pg}(TIT, T^0), c_{pcj}(TIT, T^0)]$$

TIT is a relevant temperature because it relates the overall coolant mass flow to the inlet hot gas mass flow entering the gas expander and the coolant temperatures to the firing temperature.

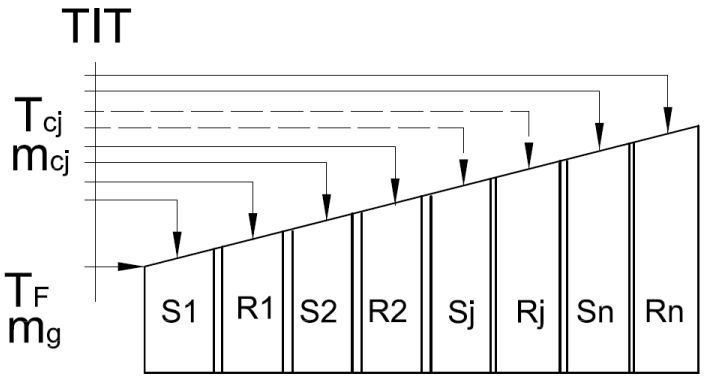

Fig. 3: Turbine Inlet Temperature Nomenclature

3 GT Global Model for the evaluation of the overall cooling mass flow

Taking results of the uncooled equivalent Brayton cycle calculation as well as the technological level (Class) of the Gas Turbine into consideration, the overall coolant mass flow required to perform the cooling purposes can be evaluated by the adoption of global models. Such models relate the overall coolant mass flow to some relevant temperatures (compressor outlet temperature, metal temperature, firing temperature that is strictly related to the TIT), to the compressor inlet or expander inlet mass flow, to the main flow and coolant flow properties and to some parameters that well represent the Class of the Gas Turbine (introduction of some coefficients).
The overall coolant flow can be express as a function of such parameters:

$$mc = f(m_g, c_{pg}, c_{pc}, T_b, T_f, T_{cex}, k_1, k_2, ...)$$

For the preliminary evaluation of the overall coolant mass flow, the coolant temperature Tc has been assumed in the range of some 400-500 °C and the blade temperature Tb in the range of 830-895 °C. Such temperatures are defined arbitrarily as reference lumped temperatures of the RO3 GT global model. In table 5, evaluation of the overall coolant mass flow for the extreme values of the coolant temperature and blade temperature is reported:

Table 5: Evaluation of the overall coolant mass flow for various coolant and blade temperature, respectively

mc	165	kg/s			
cpc	1.1	kJ/(kgK)			
mg	523	kg/s			
cpg	1.3	kJ/(kgK)	mci	685	kg/s
Tcexit	400	°C	mc/mci	24.1	%
Tf	1440	°C			
Tb	830	°C			
k1	0.1884	#			
k2	1	#			

mc	215	kg/s			
cpc	1.1	kJ/(kgK)			
mg	523	kg/s			
cpg	1.3	kJ/(kgK)	mci	685	kg/s
Tcexit	500	°C	mc/mci	31.4	%
Tf	1440	°C			
Tb	830	°C			
k1	0.1884	#			
k2	1	#			

mc	129	kg/s			
cpc	1.1	kJ/(kgK)			
mg	526	kg/s			
cpg	1.3	kJ/(kgK)	mci	685	kg/s
Tcexit	400	°C	mc/mci	18.8	%
Tf	1440	°C			
Tb	895	°C			
k1	0.1884	#			
k2	1	#			

mc	162	kg/s			
cpc	1.1	kJ/(kgK)			
mg	526	kg/s			
cpg	1.3	kJ/(kgK)	mci	685	kg/s
Tcexit	500	°C	mc/mci	23.6	%
Tf	1440	°C			
Tb	895	°C			
k1	0.1884	#			
k2	1	#			

By the assumption of some coefficients taken for the SoA, the overall coolant mass flow has been calculated and by averaging these results, an overall value is of some 26% of the compressor inlet mass flow:

$$\sum_j m_{cj} \approx 26\% \, of \; inlet \; compressor \; mass \; flow$$

Evaluation of the overall coolant mass flow given by the RO3 model leads to a value of that mass flow that agrees with the coolant ratio (m_{cool}/m_{compr}) founded in the technical background. Accordingly, in the present State of the Art models similar to that of RO3 research group has been found and evaluation of the overall coolant flow gives result not far from the RO3 calculated.

In the paper [13] a similar approach of that presented by RO3 has been found. Coolant mass flow is evaluated, according to the GT sketch given in figure 4, as a function of relevant temperature, properly coefficients and mass flows:

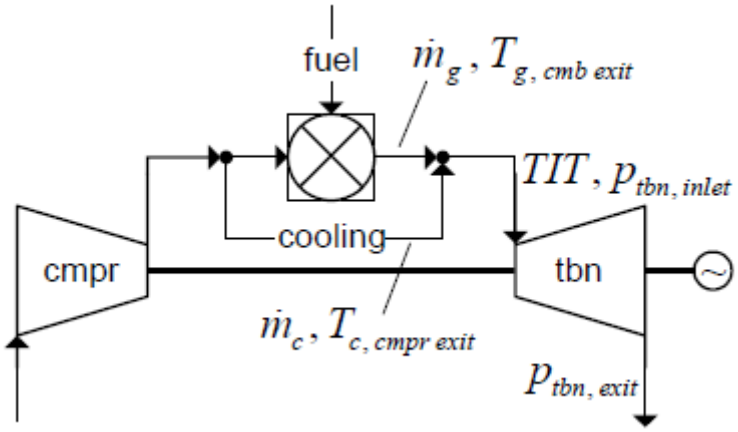

Fig. 4: Sketch of the GT presented in the paper [13]

The paper states:

The parameters b and K were adjusted to yield a net efficiency of 38.50 % at a combustor exit temperature of 1425 °C with a cooling fraction of 22 %. … The cooling fraction is the cooling fluid mass flow rate divided by the compressor inlet mass flow rate…

$$\frac{\dot{m}_c c_{p,c}}{\dot{m}_g c_{p,g}} = b\left(\frac{T_{g,\,cmb\ exit} - T_b}{T_b - T_{c,\,cmpr\ exit}}\right)^s$$

Fixed values			
$\Delta p_{cmpr,\,inlet}$ & $\Delta p_{tbn,\,exit}$ [mbar]		10	
PR [-] (base case)		17	
$\eta_{p,\,cmpr}$ [%]	91.5	T_b [°C]	860
cmb heat loss [%]	0.2	η_{mech} [%]	99.6
Δp_{cmb} [%]	3	η_{gen} [%]	98.5
Target values			
η_{net}=38.50 % at $T_{cmb,\,exit}$=1425 °C			
TIT (ISO)=1230 °C at $T_{cmb,\,exit}$=1425 °C			
cooling fraction[2]=22 % at $T_{cmb,\,exit}$=1425 °C			
Maximum net efficiency at $T_{cmb,\,exit}$=1350 °C			
$\eta_{p,\,uc\ tbn}$ [%]		89	
Tuned parameters			
b [-]	0.1884	K [-]	0.237
$\eta_{p,\,uc\ tbn}$ [%]	87.94	s [-]	1

Values similar to that established by RO3 have been found in other papers:

The turbine introduces few cycle modeling problems. For example, Reynolds number effects are small and can safely be ignored. The main concern is to achieve proper representation of the bleed flows in cooled turbines. In modern, high temperature engines, the cooling bleeds are extracted from the compression system at two or more points and returned to the cycle at several points through the turbine system. Up to 25% of the core entry flow may be used in this way. The flows provide cooling for two or more nozzle guide vane rows, at least one and probably two rows of rotor airfoils, and the front and back faces of the associated rotor discs. The bleed in-flows have complex effects on the turbine aerodynamics due to flow disturbance, boundary layer thickening, etc. Turbine specialists using a mix of CFD and empirical methods can estimate these effects. Typically, in-engine aerodynamic turbine efficiencies are some 2% lower than might be measured on a cold turbine rig, with no simulation of the cooling flows.

Moreover, in the paper of Ashok Rao., 2010, '1.3.2 Advanced Bryton Cycles' the overall coolant mass flow is related to some relevant quantities:

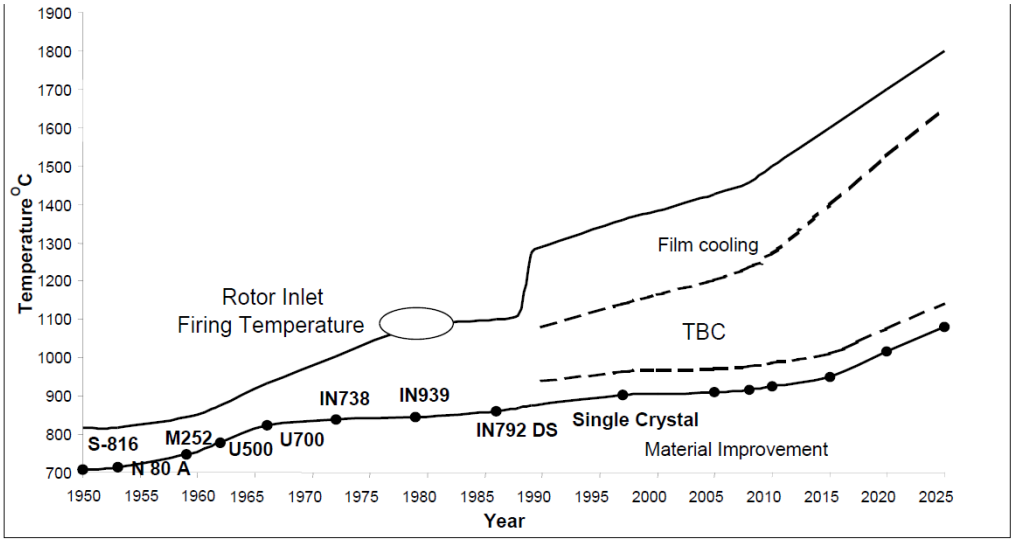

Fig. 2. Impact of Firing / Metal Temperature on Efficiency

The paper states:

In a state-of-the-art air-cooled gas turbine with firing temperature close to 1320ºC (2400ºF), as much as 25% of the compressor air may be used for turbine cooling, which results in a large

parasitic load of air compression. In air-cooled gas turbines, as the firing temperature is increased, the demand for cooling air is further increased. …

4 Heat transfer scheme and cooling scheme

Various heat transfer phenomena have to be taken during the design of the cooling system into consideration. Under the effect of convection, radiation and conduction the heat of the main stream (the hottest one) flows through the various GT components, each of them characterized by a thermal gradient. Accordingly, lot of the Gas Turbine components (disk, shroud, sidewall, blade, cavity, etc.) need to be cooled by some 'cold' air to maintain their temperature under a defined threshold value. Some coolant flows are required to achieved this purpose. Moreover, coolant flows are used for services (sealing, balance, etc.). Thus, coolant flows are not solely used for blade surface cooling, but for all the aspects concerning the GT cooling. Figure 5 represents schematically the cooling flows along a Generic 300MW F Class Gas Turbine:

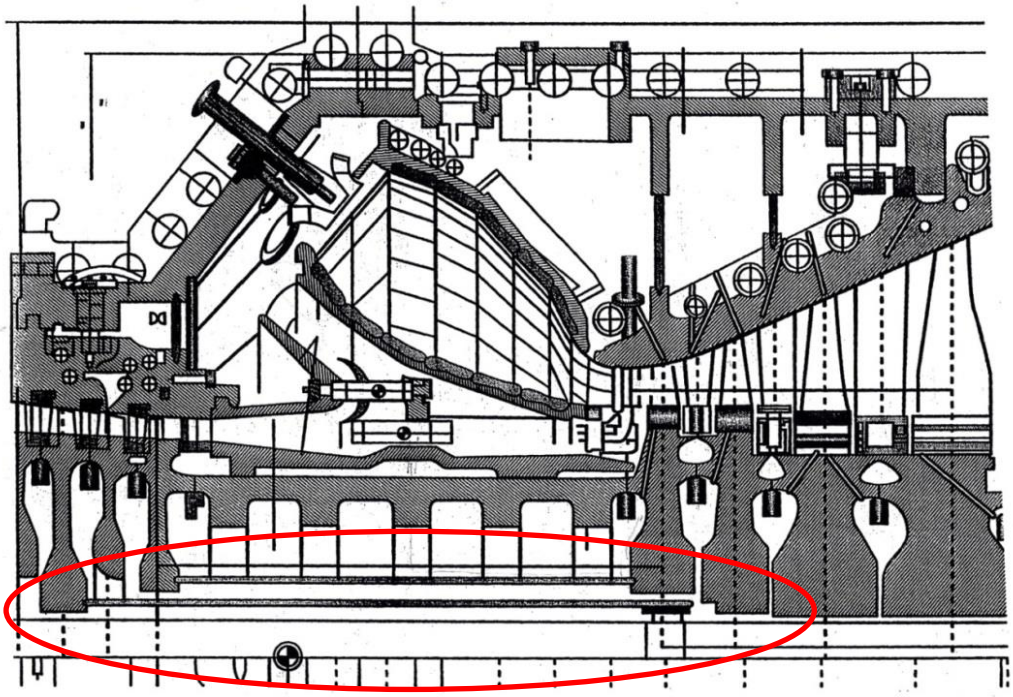

Fig. 5: Cross Section of the Cooling Paths (SIEMENS)

Moving from the 1st vane of the compressor to the last rotor row of the gas expander, the main flow path is split in various stations for various purposes, as schematically represented in fig. 5. Some fractions of the compressor inlet mass flow are extracted at different compressor stages and move to the expander stages mixing with the hot gas main flow. Main flow at the compressor exit is split in various fraction. One is directed to the 1st Nozzle Row, a second one is addressed to the 1st Rotor Row while the major of them is used for the combustion process. All the fluxes are also adopted to cool the combustion chamber externally and internally, respectively. Indeed, Combustor is also taken in the complex cooling path into consideration because of the high temperature of the combustion process. Liners of the Annular Combustor are cooled inside where the flame or combustion occurs. The inner of the liner is cooled by film and also the Liner Metal Temperature (LMT) is reduced by the interposition of the Thermal Barrier. The outer of the combustor is protected by the coolant

flows directed to the 1st expander stage. The extracted mass flows, both from the compressor stages both at the combustor inlet, are not used for the 100% to the surface blade cooling but also for other features.
As an example of the high complexity of the heat transfer phenomena occurring in the Gas Turbine, in figure 6 a sketch of the heat fluxes moving from the combustion chamber to the casing and to the shaft is given:

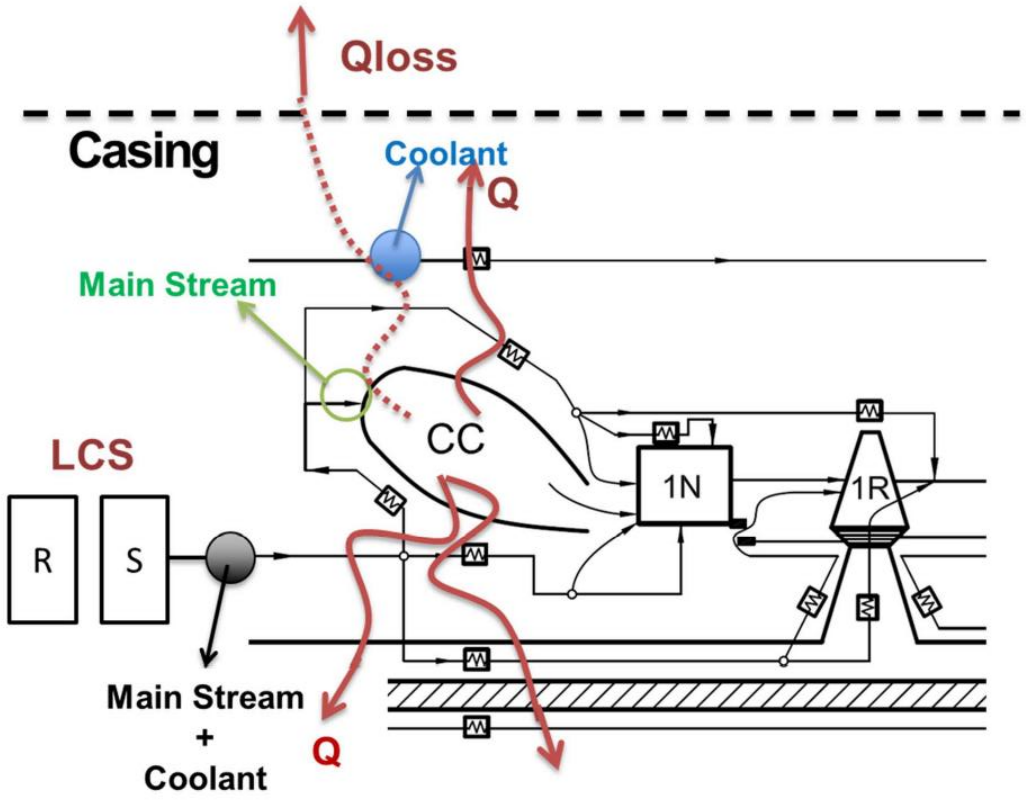

Fig. 6: Schematic View of the main stream and coolant streams along the combustor and of the heat fluxes moving through the GT to the casing and to the inner components (shaft, disk, etc.)

Convection, radiation (especially for the combustion chamber) and conduction phenomena have to be taken for the GT cooling into account. Indeed, high temperatures are reached during the combustion process so systems to maintain the component temperature under a threshold upper limit are usually adopted. Both the coolant flow addressed to the expander and the main flow sent to the burner lap the outer surface of the liner, while the inner of the liner is cooled by film and also the Liner Metal Temperature (LMT) is reduced by the interposition of the Thermal Barrier. Even if the complex system of the combustion chamber is cooled, some heat fluxes flow through the metal to the casing and to the shaft, respectively. Taking the outer (casing) and the inner (disks, shaft, etc.) components of the machine into account, main flows and coolant flow are subjected to convection and radiation heat transfer phenomena. According to figure 6, these streams increase their temperatures moving along the combustor.

4.1 Flow in the Expander Stages

Description of the purposes that the coolant flows has to perform allows to better understand which peculiarities of the GT cooling are taken by the RO3 Lumped Model into account. According to figure 5, the 'cooling channels' of the compressor rotor rows extractions are highlighted by the red circle. This channels lead the coolant flows to the respectively expander stages in order to cool all the components thermally stressed.

List of the main row components that required to be cooled to maintain their temperatures under the threshold value is given and by the help of some exemplificative pictures the expander flow paths are described.

- Disk
- Disk Cavity
- Shroud
- Platform
- Shank
- Sidewall
- Airfoil Surface
- Tip Cap
- others

Moreover coolant flows are used for the services. Such a services are as an example the piston balance, the sealing and other as shown in figure 7 below:

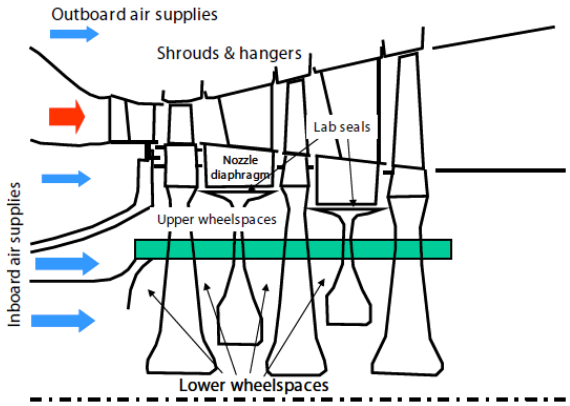

Fig. 11. Heavy Frame Turbine Secondary Flow Regions

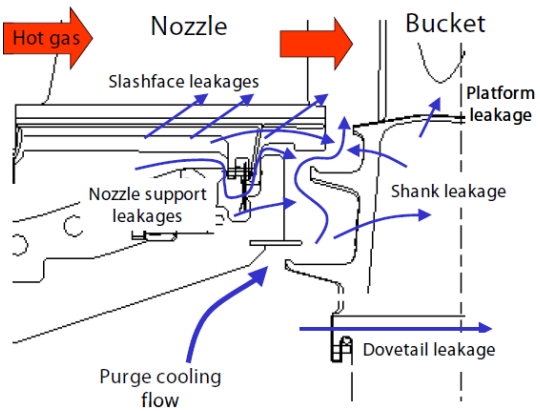

Fig. 13. Cooling Flows and Leakages in Buffer Cavity Region

Fig. 7: Schematic view of the cooling paths along the disks – As example

Coolant mass flows extracted from the compressor stages have different paths and are addressed both for stator row and for the rotor row. By the simplified adoption of Fig. 8, is possible to better understand which are the various coolant flow paths along the gas turbine.

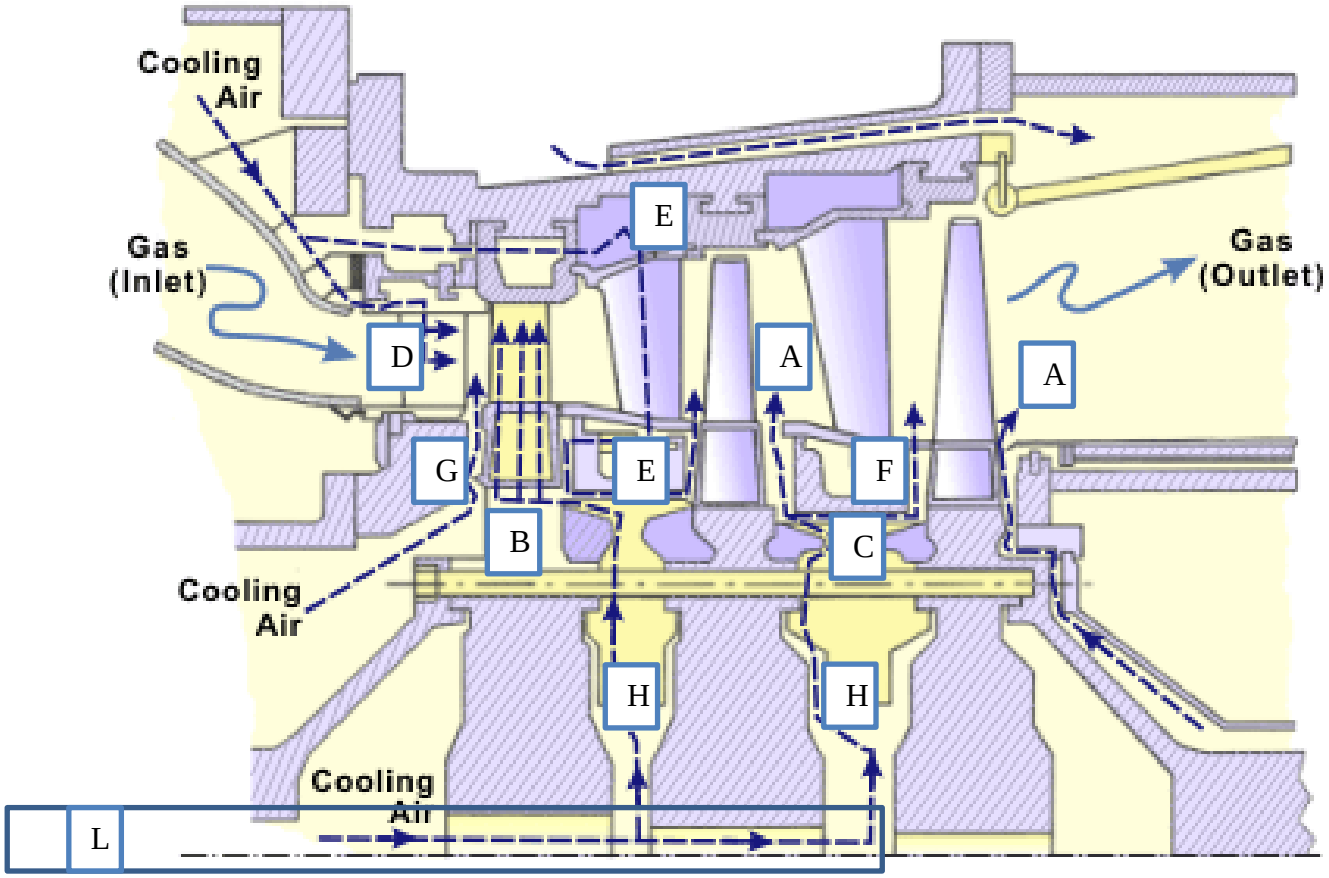

Fig. 8: Example of a Generic Gas Turbine Cooling Path along Stator and Rotor Row

The path from the extraction (bleeding) sections to the respectively expander rotor row is the cooling passage represented by **L** in Fig. 8.
The coolant flows pass through the shaft before entering the disk cavity and the disk.

Bleed extractions addressed to the stator (nozzle) rows pass externally (around) the machine lapping the case before re-entering in the respectively row.

The coolant flow addressed to a Stator Row assuming the schematization of Fig. 8 is used for various purposes:

- Cooling of the Airfoil Surface (inner and outer) - **D** in the Fig. 8
- Cooling of the Platform and Sidewall (inner and outer) - **E** in the Fig. 8
- Mixing with the main stream, downstream the Stator Vane - **G** in the Fig. 8

Extracted mass flow for the Stator Row cooling is used for various cooling surfaces. For this reason the overall extracted mass flow is split in various fractions, adopted for the various cooling purposes, respectively. A schematic view of the Stator Row cooled components is given in Fig. 9:

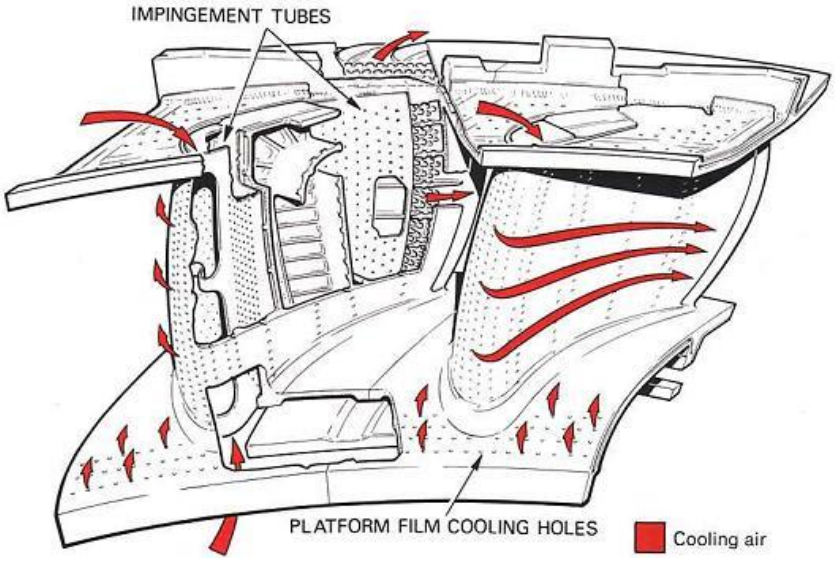

Fig. 9: Schematic View of the Cooled components of the Stator Row – As Example

As for the Stator Row also for the Rotor Row, coolant flows are used for various row components cooling and the overall mass flows (extracted from the compressor) are divided into minor flows for different purposes:

- Cooling of the disk outer – **H** in the Fig. 9
- Cooling of the Airfoil Surface (inner and outer) - **B** in the Fig. 9
- Cooling of the Shank - **C** of Fig. 9
- Sealing - **F** in the Fig. 9
- Mixing with the main stream, downstream the Rotor Blade – **A** in the Fig. 9

From the Rotor Blades, heat fluxes move to the shaft passing through the various components. A typical temperature distribution along the disk is given in Fig. 10:

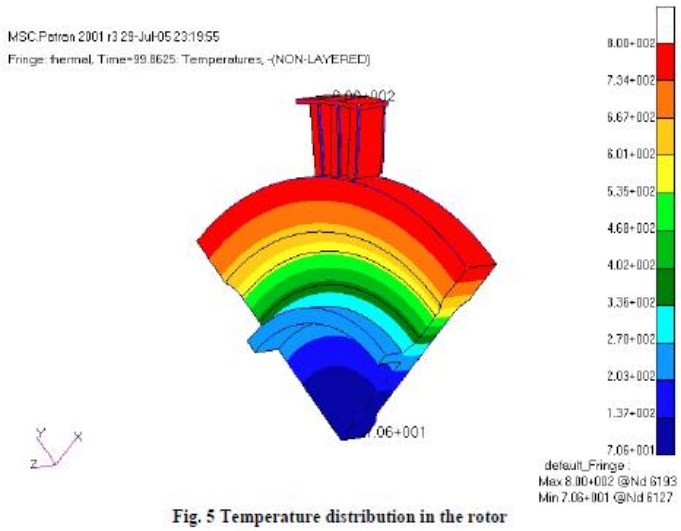

Fig. 10: Typical Temperature Distribution along a 1st Stage Aeronautic Rotor Disk – As Example

All these aspects (components cooling, services, sealing, etc.) have to be considered to evaluate the coolant mass flows and the various temperatures of the phenomena. Indeed, heat removed from all the hot components (disk, shank, etc.) flows towards the fractions of the overall coolant flow designed to perform the defined purpose (cooling, service, sealing, etc.).
To ensure that all the temperature of the various components are sufficiently lower than the threshold value, the bled mass flow is split in various fluxes. A first assumption for all the Stator Rows, except for the first one, is that a 60% of the overall coolant flow is addressed to the blade surface cooling and the other 40% is used for the sidewall, platform and for all the other components previously described. In Fig. 11 a detailed figure of the Stator (Nozzle) Row cooling components is given:

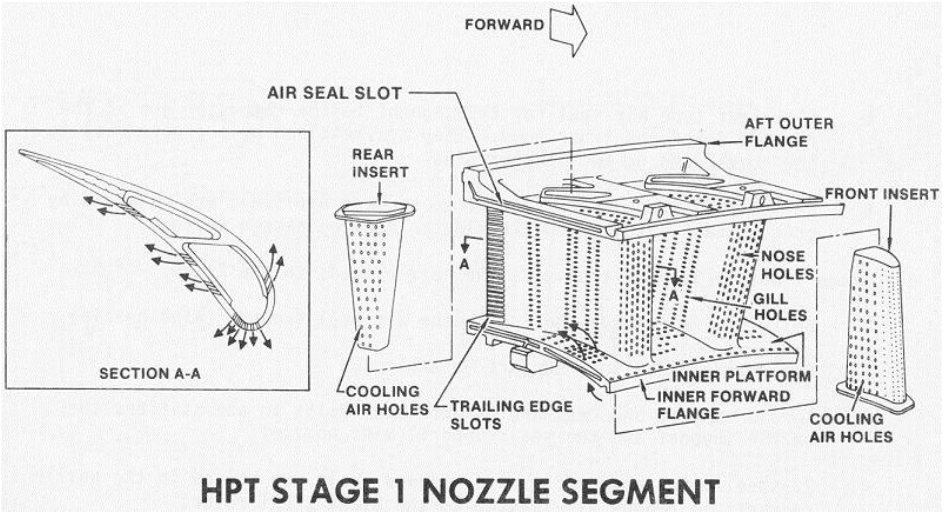

Fig. 11: Schematic View of a 1st Nozzle Vane Cooling Components – As Example

Coolant mass flows distribution for the Rotor Rows is pretty similar to the Stator Row. Some 65% of the overall extracted coolant flow is used for the blade surface cooling and the rest some 35% is addressed to the other row components (dovetail serration, shank, platform, etc.). In Fig. 12 a detailed representation of a Rotor Blade cooling components is given:

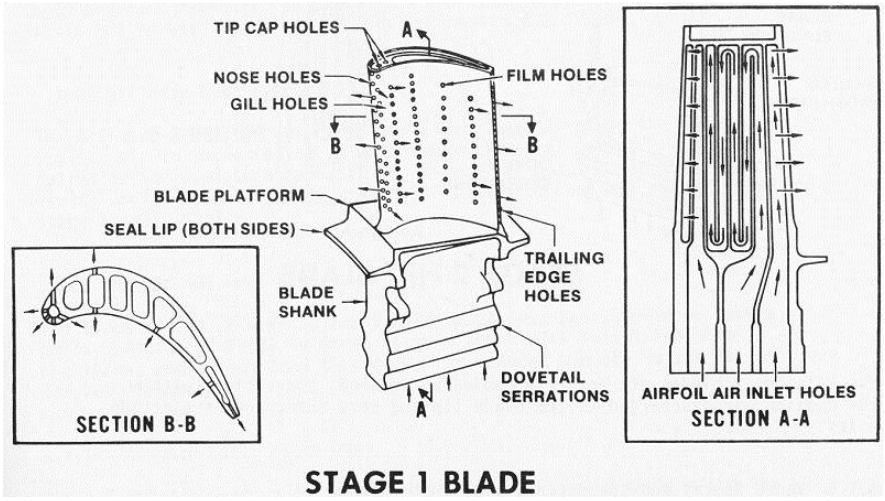

Fig. 12: Schematic View of a 1st Rotor Blade Cooling Components – As Example

Of course even if the stator row and the rotor row blades of the last expander stage are uncooled (not cooled by internal coolant flows and not film cooled). Some coolant flows are addressed anyway to that stage because the disks have always to be cooled. Thus a heat flux from the hot parts to the cold one exists. In figure 13, a schematically comparison of the various coolant flows between the cooled blade and uncooled blade is sketched. Moreover, the RO3 GT cooling model is schematically represented in figure 14.

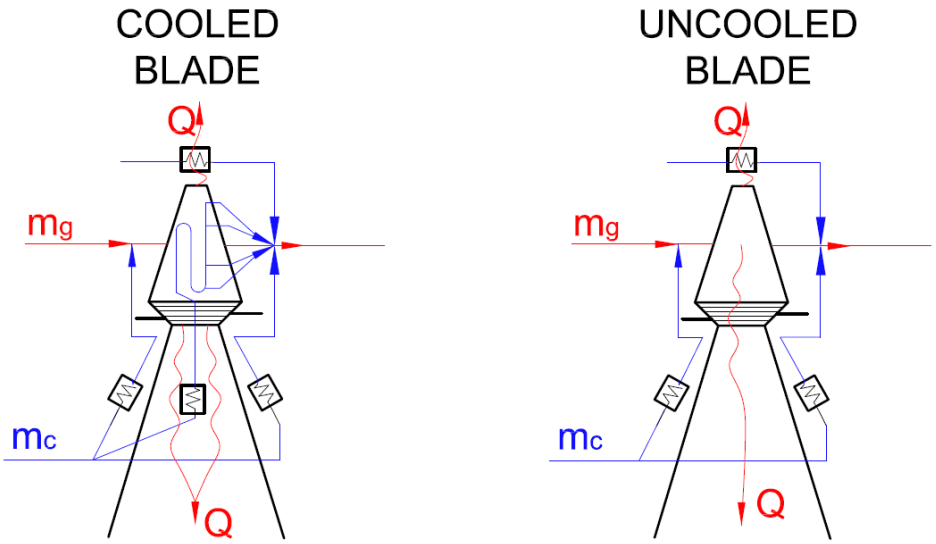

Fig. 13: Comparison between cooled blade and uncooled blade coolant flow

Each Heat transfer process is characterized by a '*heat transfer effectiveness'* if a Effectiveness - Number of Transfer Unit (ε-NTU) approach is adopted to model the GT cooling system. Taking the various heat transfer phenomena characterized by a certain effectiveness into account, the coolant flow fraction distributions has been evaluated according to the above:

Table 6: Fractions of the overall mass flow for each row (in percentage %)

Coolant Mass Flow Percentage % for the various purposes								
STAGE	1st Stage		2nd Stage		3rd Stage		4th Stage	
ROW	1S	1R	2S	2R	3S	3R	4S	4R
Airfoil Surface	50	65	60	65	60	65	0	0
Other Purposes (endwall, shroud, sealing, etc)	30	35	40	35	40	35	100	100
Jet Cooling	20	0	0	0	0	0	0	0

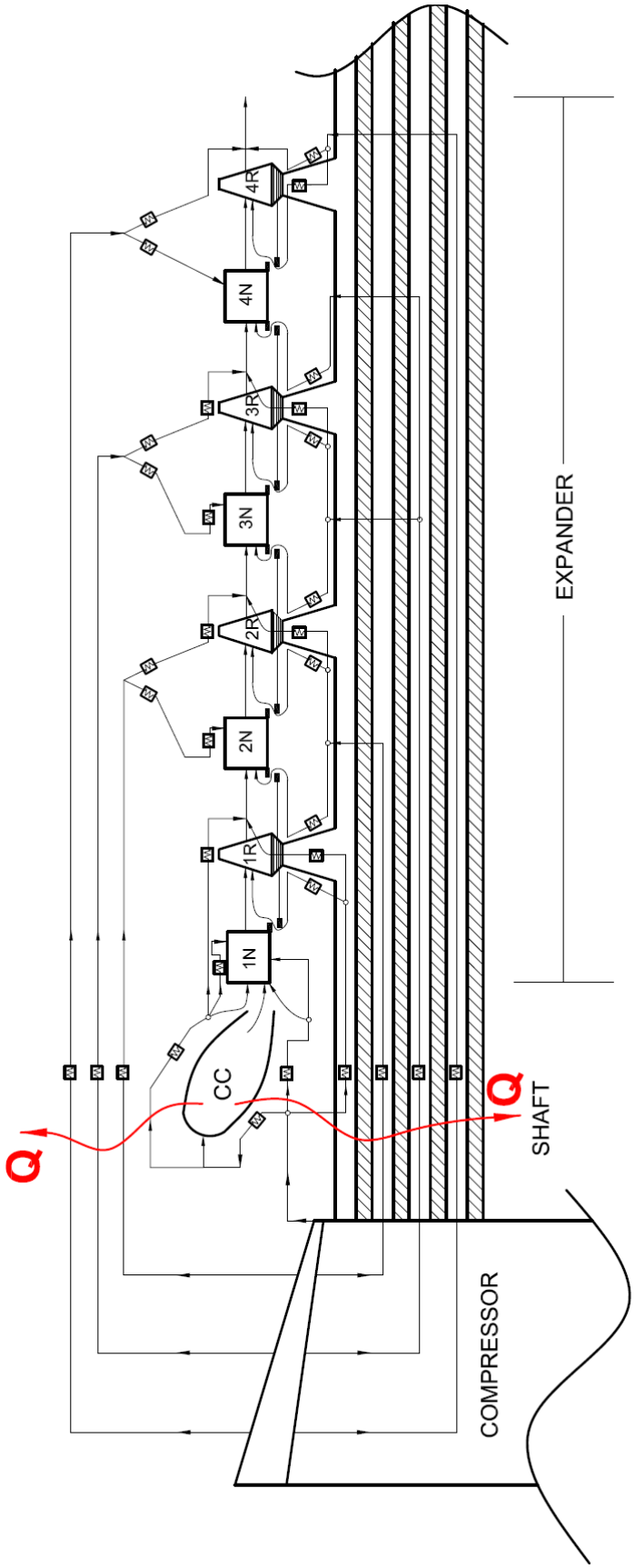

Fig. 14: Schematic View of the cooling path
from the compressor bleeding station to the expander row injection station

5 Lumped Performance Features Model

According with the Deliverable 4.2.2, RO3 modelling approach is based on a FV lumped feature and performance discretisation of components. The approach is addressed to model any kind of machines and apparatuses made of elementary components such as: compressor rows, expander rows, combustion chambers, heat exchangers, pumps, etc. Real three dimensional time dependent measured flow features are taken into account by lumping on the *FV* boundary models J and $J+1$ the distributions of quantities of interest such as pressure, velocity, temperature, etc., by means of an averaging procedure on surface and time. Moreover the lumping procedure is adapted for the quantities that are involved in the component performance calculation according to the implemented modules. The lumped features are reduced to the *FV* central nodes J_N.

This approach can be easily adopted for a heat transfer device. The Gas Turbine cooling system can be seen as a complex arrangement of series and parallel heat transfer devices. Heat transferred from a fluid to the other (the performance) is related to the lumped flow features and to the geometric features of the various components by adapting classical heat transfer model. The connection between component features and heat transfer model is established according to the amount of data available by detailed simulations. As an example both shell and tube and finned tube heat transfer device lumped scheme is given in figure 15a –b:

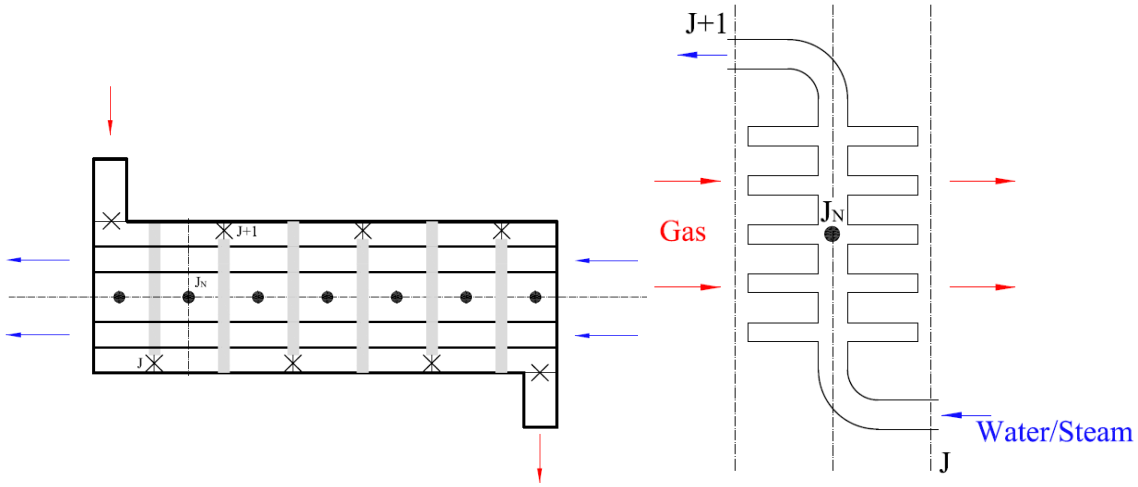

Fig. 15 a-b: sketch of the lumped approach for heat transfer devices

Accordingly, RO3 University Simulator takes a GT cooling lumped model into account which implies transfer of heat from the main flow (hot gas) to the coolant flows, through various components (blade row, disk, etc.). Moreover, some heat flows from the hottest GT components (i.e. combustion chamber) to the colder ones (i.e. shaft, casing, etc.). Taking the description of the cooling paths along the machine into consideration, in such a lumped model the coolant flows consider both the airfoil blade cooling and the cooling of the other parts (disk cavities, shrouds, endwalls (sidewall) and the action of coolant as sealant flow re-entering into the main flow. Temperatures (coolant, blade, etc.) have the meaning of lumped reference temperature of the complex cooling process.

6 Blade Cooling Model

Gas Turbine Blade Cooling can be seen as a series of layers characterized by different heat transfer phenomena. In figure 16 sketch of that schematization is depicted:

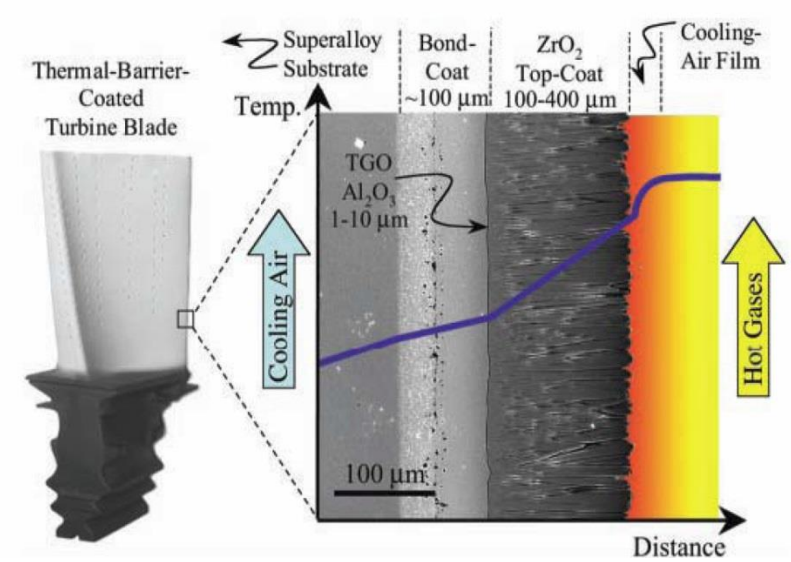

Fig. 16: Sketch of a Rotor Blade temperature distribution along the layers

Moving from the inner side (coolant) to the outer one (main stream) the following heat transfer layers can be described:

- Internal Cooling Flow → Bulk Material: convection heat transfer

  Coolant mass flow entering the blade is used to remove the heat flowing from the metal. Flow velocity, gas composition, architecture and geometry of the blade are some parameters that influence the internal convection heat transfer phenomena.

- Bulk Material and Thermal Barrier Coating: conduction heat transfer

  Both for the Bulk Material (BM) and for the Thermal Barrier Coating (TBC) the heat flux coming from the outer surface passes through the various conductive layers characterized by a thickness s_j and by a thermal conductivity λ_j, that is a function of the heat transfer temperatures.

- Thermal Barrier Coating→ Hot gas: prevalent convection heat transfer

  The hot gas exiting the combustion chamber and entering the expander is at high temperature. The model takes both the radiation effects and the convection into account by considering the heat transfer as a prevalent convection phenomena.
  By the adoption of the most suitable expression, the hot gas prevalent convection heat transfer coefficient U_g can be evaluated:

$$Nu = A \cdot \mathrm{Re}^m \cdot \mathrm{Pr}^n \cdot \left(\frac{T_g}{T_W}\right)^q \qquad (1)$$

Nu being the non-dimensional group of Nusselt, , *Re* being Reynolds number, *Pr* being Prandtl number, T_g being the gas temperature, T_W being the wall temperature and *A*, *m*, *b*, *q* coefficients depending on the phenomena. By the adoption of different value of these coefficients also internal convection heat transfer coefficient U_{c0} can be evaluated.

The various heat layers can be seen as a thermal equivalent circuit and schematically the heat transfer phenomena previously described can be represented as a series of thermal resistance as shown in the figure 17:

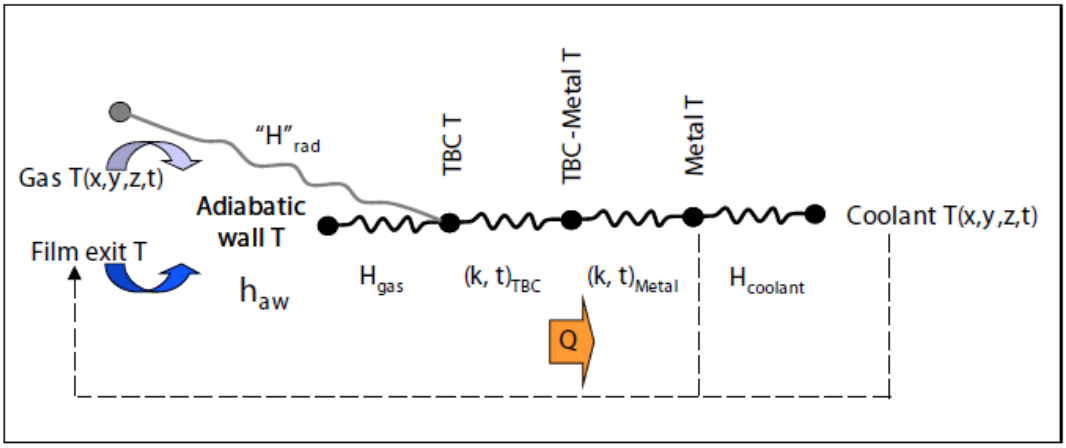

Fig. 6. General Thermal Resistance Model

Fig. 17: Simplified view of the thermal resistance for a generic blade

To improve the performance of the blade in term of rate of life consumption is desirable to increase the outer thermal resistance (reduce the external heat transfer coefficient), to reduce the inner thermal resistance (increase the internal heat transfer coefficient) and to adopted a thermal barrier coating layer characterized by an high thermal resistance (high conductivity). Various techniques are employed both on cold side and on the hot side to better remove the heat from the blade.

On the coolant flow side, adoption of some architectural devices as the turbulence promoter, the rib arrangement, the pin fins and of jet impingement technique leads to increase the internal heat transfer coefficient. Each enhancing system can be seen as a corrective coefficient f_{jk} greater than 1 of the equivalent smooth heat transfer coefficient U_{c0}. Accordingly, in figure 18 temperature profile modification on the coolant side owing to the enhancing system of the heat transfer coefficient is given:

- jet impingement → f_{ji} >1
- turbulence promoter → f_{tp} >1
- rib arrangement → f_{tp} >1
- pin fins → f_{pf} >1

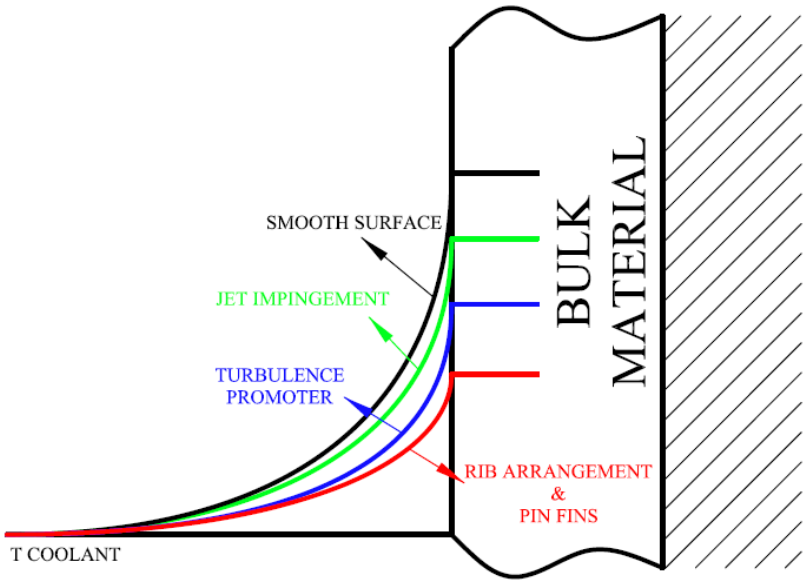

Fig 18: Schematic view of the enhance system of the internal heat transfer coefficient

Turbulence promoter are widely employed in Heavy Duty Gas Turbine inner channels in order to enhance the internal heat transfer coefficient. Taking ribs configuration according to Data Base (figure 19-a) into consideration, in figure 19-b the increase of heat transfer coefficient is shown.

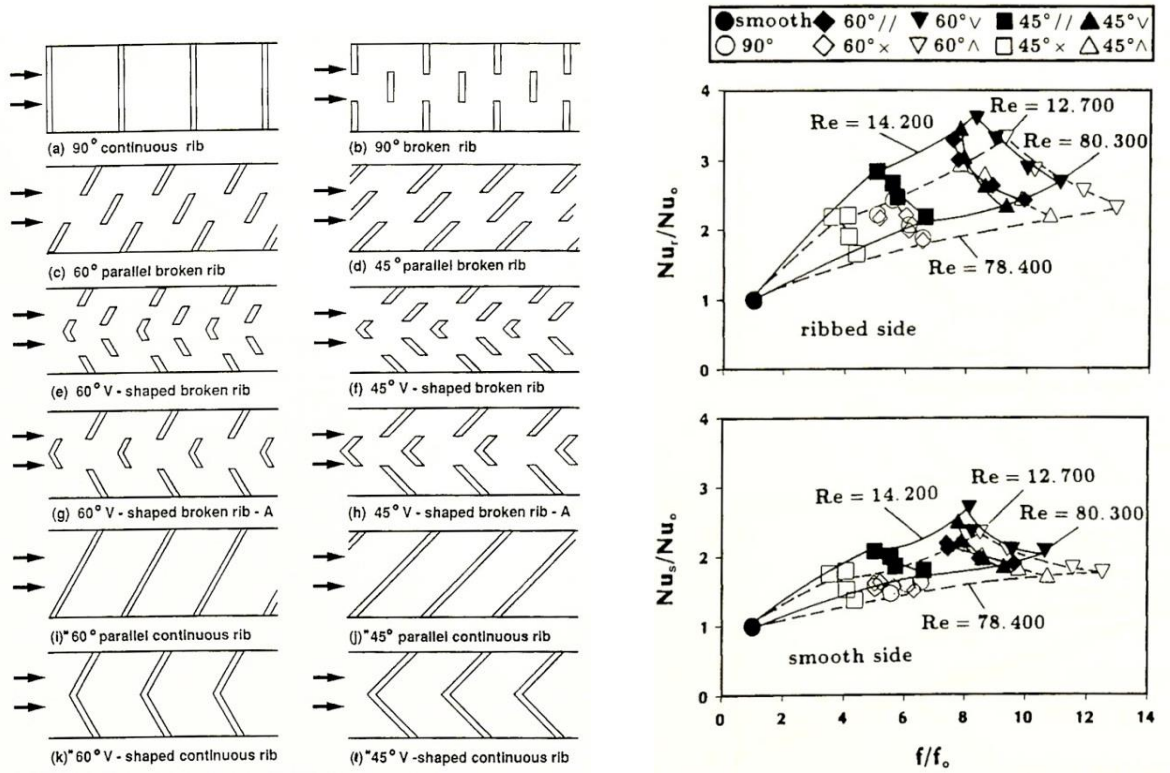

Fig. 19 a-b: a) rib distribution – b) Influence of Turbulent promoter on the NU number

Adoption of impingement concepts leads to enhance the internal heat transfer coefficient. The overall increase of the Nusselt number depends on many architectural and geometrical parameters taken from Data Base and from the HDGT State of the Art. Nusselt non-dimensional group versus some architectural ratios is shown in figure 20:

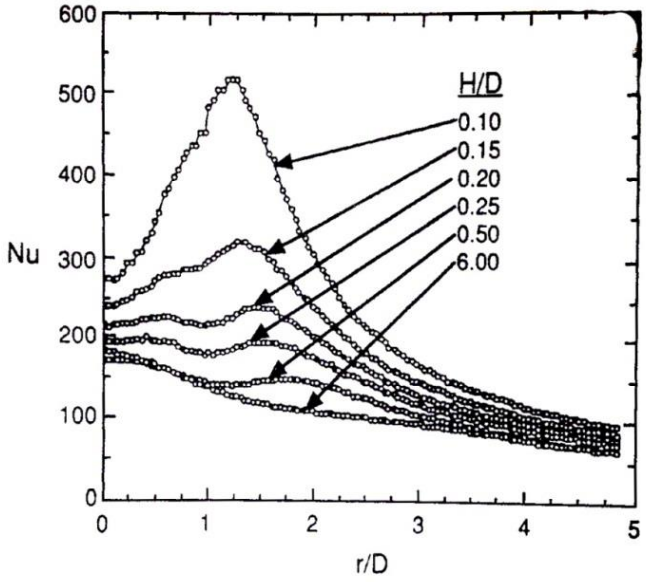

Fig 20 : Influence of jet impingement architecture on internal heat transfer coefficient

Heat flux coming from the blade layers is mitigated by the coolant mass flow taken from compressor. Internal heat transfer coefficient U_{c0} is evaluated taking internal diameter, velocity, mass flow, viscosity, etc. into account. Internal devices, suitably arranged (pins, rib, etc.) as well as the jet impingement are designed to enhance internal heat transfer coefficient.
Coolant mass flow passes through multi-pass channel, increasing the effective surface of the heat transfer, before exiting from the blade and mixing with the main hot gas stream. The contribution of turbulence promoters, ribs arrangement, pin fins and jet impingement are taken into account by expressing the coolant heat transfer coefficient:

$$U_c = U_{c0} \cdot f_{Tp} \cdot f_{ji} \cdot f_{ra} \cdot f_{pf}$$

On the other side, the hot one, introduction of techniques to reduce the external heat transfer coefficient are taken into consideration. The adoption of film cooling allows to depress the hot gas heat transfer coefficients (U_{g0}) by the correction of a f_{film} coefficient, lower than 1, because of the cold insulating layer between the hot gas stream and the wall of the blade.
Accordingly, film cooling can be also seen as an additional thermal resistance layer characterized by an equivalent thickness and thermal conductivity. In figure 21, temperature profile with and without film cooling is depicted:

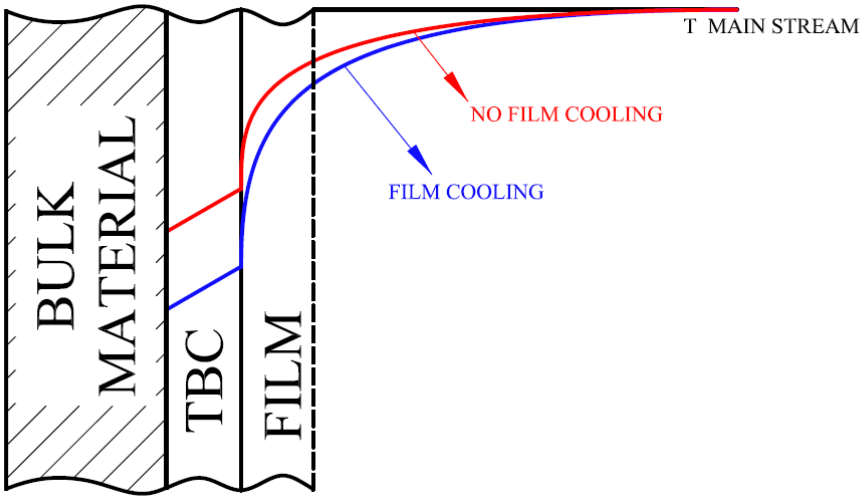

Fig 21: Schematic view of the depression of the external heat transfer coefficient owing to the film cooling

Main stream prevalent convection heat transfer coefficient U_{g0} is related to some parameters such as velocity, efflux area, conductivity, viscosity, etc. External heat transfer coefficient assumes different values for different points among the blade profile as shown in fig.22. By the adoption of RO3 lumped model hot gas heat transfer coefficients have been evaluated for the various blade rows. When the film cooling occurred, external heat transfer coefficient is depressed by the coolant mass flow exiting from the blade row holes realizing a thin cold film that protects the blade.

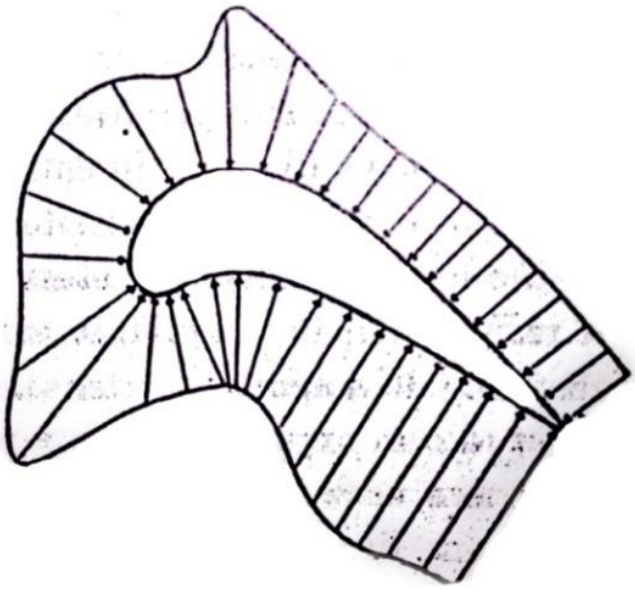

Fig. 22: Typical heat transfer distribution among the blade row surface

Heat transfer coefficient distribution on pressure and suction side and film cooling influence on the phenomena are shown in figure 23:

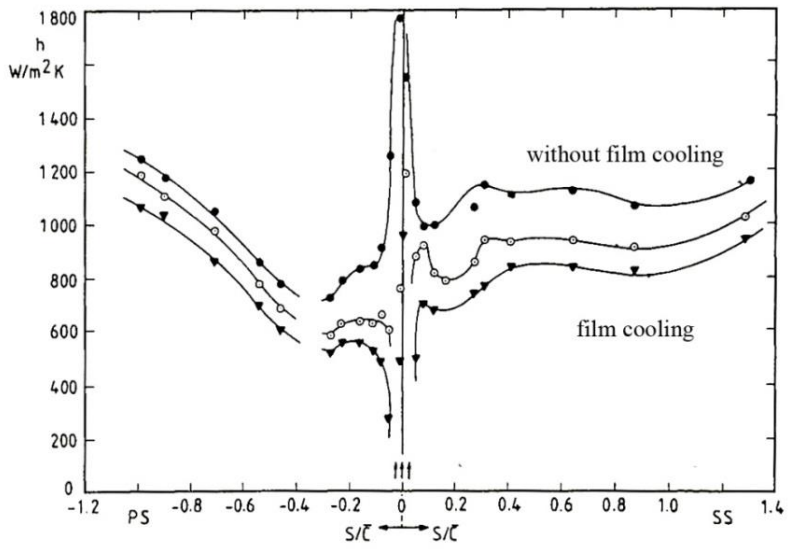

Fig. 23: External heat transfer coefficient depressed by the film cooling

The hot gas heat transfer coefficient can so be expressed:

$$U_g = U_{g0} \cdot f_{film}$$

$f_{film} < 1$ being the film cooling coefficient.

Also BM and TBC layer influences the heat transfer process. Bulk Material and Thermal Barrier Coating thermal resistances are evaluated taking the thickness s_j and the thermal conductivity λ of the layer into account. Changing the thickness of the TBC layer and the TBC material composition, the coolant mass flows required to maintain the same ratio of life consumption change significantly. As an example, in figure 24 modification of the coolant flows versus the TBC thickness is presented:

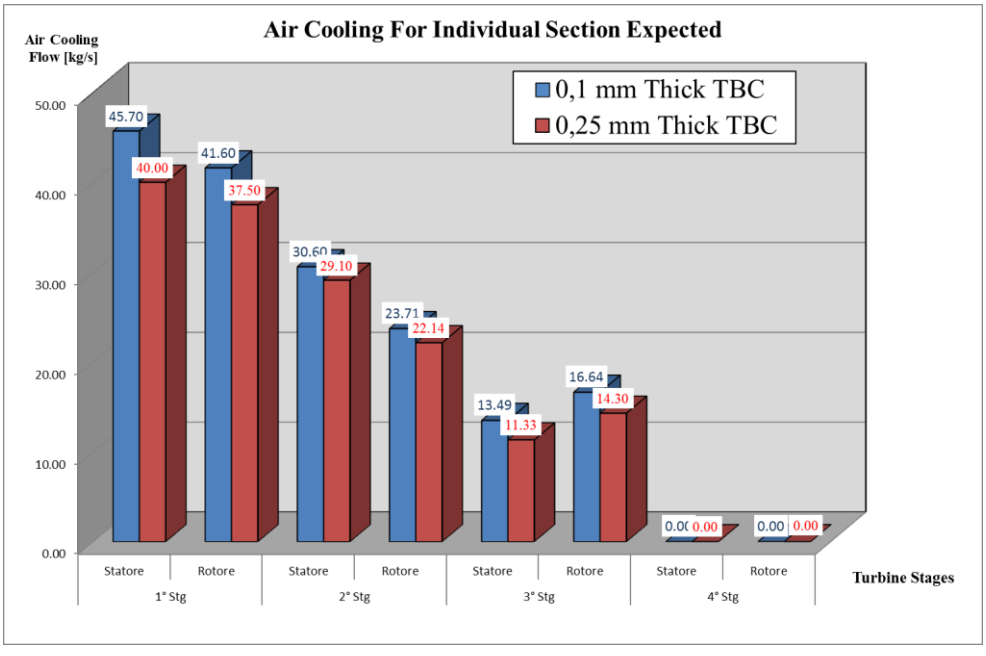

Fig. 24: Influence of the Thickness TBC layer on the coolant flows

6.1 Cooling Effectiveness

Combining the various heat transfer processes (phenomena) together the overall GT blade temperature profile is sketched in figure 24.

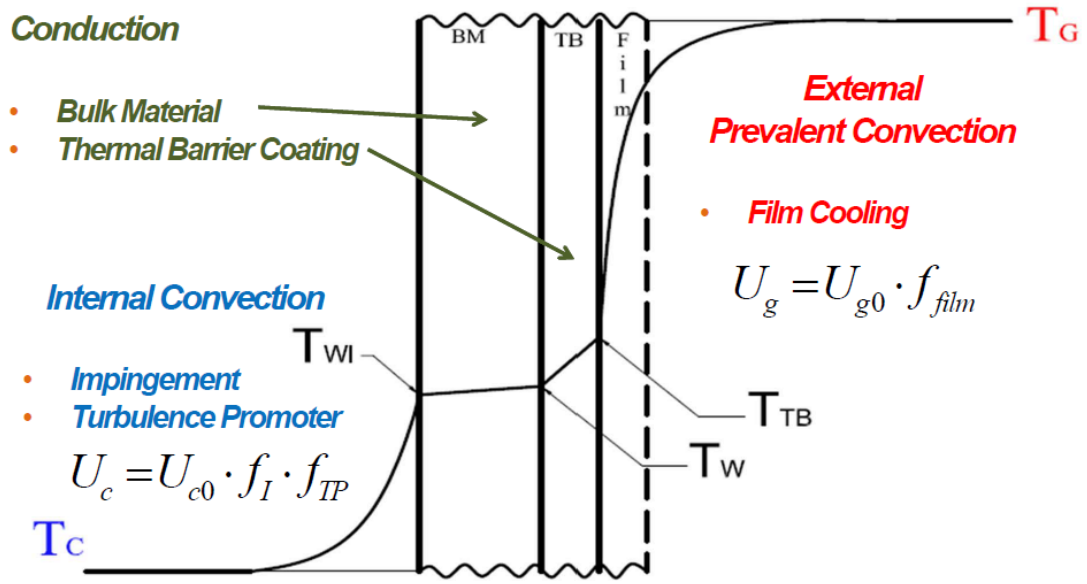

Fig. 25: Temperature profile along the various blade layers

From the technology point of view a global relationship exists between the characteristic temperatures of cooling phenomena and cooling effectiveness. For each blade row the cooling effectiveness can be expressed:

$$\eta_c = \frac{T_g - T_W}{T_g - T_c} \qquad (2)$$

Such a cooling effectiveness is an empirical result and is an empirically established relationship among architecture, geometry of the coolant system (platform, blade, shroud, etc.) thermic and thermal barrier, bulk material as well as main stream and coolant parameter relevant for the heat transfer process. It is a results of coupling, of a coolant stream and blade seen as an heat transfer device and of the outer stream.

6.1.2 Effectiveness – Number of heat Transfer Unit

To establish a global relation to express cooling effectiveness η_c in terms of characteristic quantities of the overall phenomena, such as coolant and hot gas mass flows, architectural and geometric parameters as well as heat transfer coefficients, the problem can be addressed by adopting the Effectiveness VS Number of heat Transfer Unit $\varepsilon - NTU$ approach.

Effectiveness represents the effective heat Q that can be exchanged versus the heat Q_∞ that could be hypothetically exchanged by a heat transfer device of infinite surface (3):

$$\varepsilon = \frac{Q}{Q_\infty} \tag{3}$$

The Number of heat Transfer Unit is expressed by the relation (4):

$$NTU = \frac{U \cdot S}{c_p \cdot m} \tag{4}$$

U being the heat transfer coefficient, S the characteristic Surface of phenomena, c_p the specific heat of the fluid and m the mass flow.
Depending on geometry, holes arrangement, streams directions (equicurrent, countercurrent) and so on, the most adequate formulation that relates ε to NTU can be adopted, taking Data Base and the State of the Art into consideration:

$$\varepsilon = f(m_g, m_c, U_g, ..., NTU, geometry, architecture) \tag{5}$$

According to nomenclature of figure 25 cooling effectiveness η_c can be evaluated as a combination of effectiveness related to elementary heat transfer processes taking film cooling, impingement, conduction and all aspects into consideration. Moreover, evaluation procedure of cooling effectiveness η_c has been performed taking relationship of counter current heat exchange from Data Base into account. Accordingly, the following heat transfer process have been described:

- Hot gas – Thermal Barrier effectiveness

$$\varepsilon_1 = \frac{\Delta T_g}{T_g - T_{TB}} = 1 - e^{-NTU_1} \tag{6}$$

$$NTU_1 = \frac{U_1 \cdot S_g}{m_g \cdot c_{pg}} \tag{7}$$

$$U_g \approx U_{g0} \cdot f_{Film} \tag{8}$$

U_g being the heat transfer coefficient of the hot stream corrected by film cooling coefficient (if film cooling is adopted) depressing the hot gas heat transfer coefficient U_{g0}. f_{Film} is lower than 1.0.

In the various gas expander row, hot gas stream reduces its temperature both because of the expansion (uncooled) and because of the injection of the coolant flows into the main stream. The latter aspect lead to a temperature difference ΔT_g strictly connected to the heat transfer process. A schematic equivalent representation, not to scale, of the cooling effect on the gas side is given in figure 26:

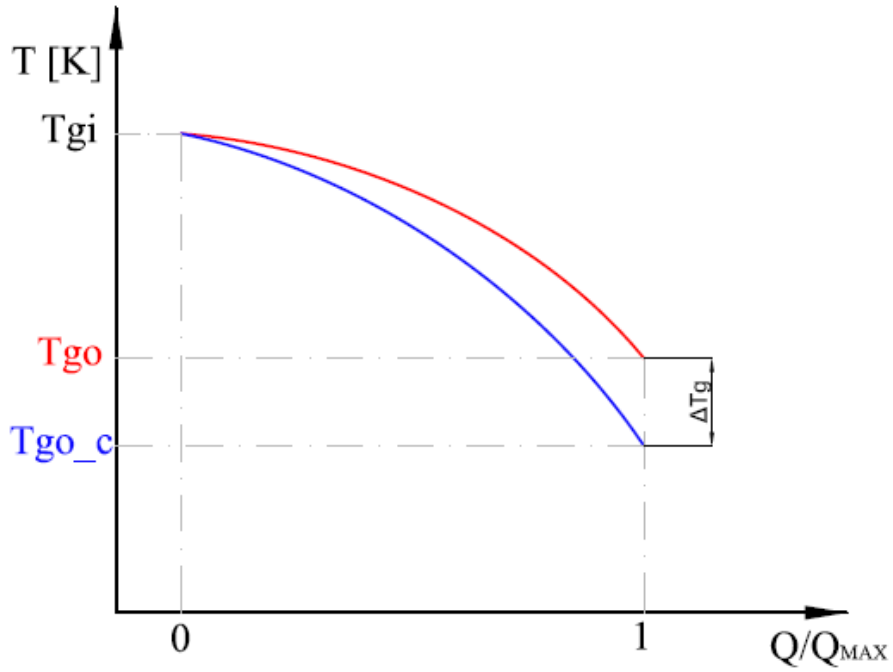

Fig. 26: schematically main stream temperature decrease – Not to scale

- Hot Gas – Bulk Material

$$\varepsilon_2 = \frac{\Delta T_g}{T_g - T_W} = 1 - e^{-NTU_2} \tag{9}$$

$$NTU_2 = \frac{U_2 \cdot S_g}{m_g \cdot c_{pg}} \tag{10}$$

$$U_2 \approx \frac{1}{\frac{1}{U_g} + \frac{s_{TB}}{\lambda_{TB}}} \tag{11}$$

U_2 being the heat transfer coefficient taking convection of the main stream and conduction of the TB layer into consideration.

- Hot Gas – Coolant

In this case two different fluids take part at the heat transfer phenomena. According to Data Base, expression of effectiveness is different from the (6) and (9) because Thermal Capacity Ratio TCR must be considered (12):

$$\chi = \frac{m_c \cdot c_{pc}}{m_g \cdot c_{pg}} \tag{12}$$

Coolant stream is the lower heat thermal capacity fluid that must be put at the dominator of NTU expression:

$$\varepsilon_3 = \frac{T_{Co} - T_{Ci}}{T_g - T_{Ci}} = \frac{1 - e^{-NTU_3 \cdot (1-\chi)}}{1 - \chi e^{-NTU_3 \cdot (1-\chi)}} \tag{13}$$

$$NTU_3 = \frac{U_3 \cdot S_i}{m_c \cdot c_{pc}} \tag{14}$$

$$U_3 \approx \frac{1}{\frac{1}{U_g} \cdot \frac{S_c}{S_g} + \frac{s_{TB}}{\lambda_{TB}} \cdot \frac{S_c}{S_g} + \frac{1}{U_{BM}} + \frac{1}{U_c}} \tag{15}$$

$U_c = U_{C0} \cdot f_{TP} \cdot f_I$ being the internal coolant heat transfer coefficient corrected by enhancing coefficient related to turbulence promoter and impingement effect, respectively.

U_{BM} being the heat transfer coefficient of the bulk material, s_{TB}/λ_{TB} being the heat transfer coefficient trough the thermal barrier.

In this simple application, expressing cooling effectiveness as (16):

$$\eta_c = \frac{T_g - T_W}{T_g - T_c} \tag{16}$$

and combining effectiveness of sub-process (9) and (13):

$$\frac{T_g - T_W}{T_g - T_c} = \frac{\varepsilon_3 \cdot \Delta Tg}{\varepsilon_2 \cdot (T_c - T_{co})} \tag{17}$$

Substituting (17) into (16), cooling effectiveness is expressed in terms of mass flows, architectural and geometrical parameters (19) taking conservation of energy into account (18):

$$m_c \cdot c_{pc} \cdot (T_c - T_{co}) = m_g \cdot c_{pg} \cdot \Delta T_g \tag{18}$$

$$\eta_c = \frac{\varepsilon_3}{\varepsilon_2} \cdot \frac{m_c \cdot c_{pc}}{m_g \cdot c_{pg}} \tag{19}$$

Finally combining (19) with (9), (12) and (13) analytic expression, for a really simple case, of cooling effectiveness η_c is obtained and given as rule (20):

$$\eta_c = \chi \cdot \frac{1-e^{-NTU_3\cdot(1-\chi)}}{1-\chi\cdot e^{-NTU_3\cdot(1-\chi)}} \Big/ \frac{}{1-e^{-NTU_2}} \qquad (20)$$

Such an effectiveness depends on many parameters and empirically known aspects:

$$\eta_c = f(m_g, c_{pg}, m_c, c_{pc}, U_i, U_o, \lambda_j, s_j, architecture, geomtry, etc....)$$

Accordingly, RO3 GT Cooling model based on lumped performance features includes all the aspects previously described (airfoil, platform, sidewall cooling and others). The best fit relation to establish the cooling effectiveness (taking architecture, technology, flow feature, etc. into account) can be described by the following equation:

$$\eta_{cj} \approx \chi \cdot k_1 \cdot e^{-k_2\cdot\chi} \qquad (21)$$

k_1 and k_2 being coefficients taking cooling modern technologies into account.

By the adoption of this expression of the Cooling Design curves, the coolant flow for each stator row and rotor row, respectively, can be established. In figure 27, such RO3 curves for a generic stator row and a rotor row are given:

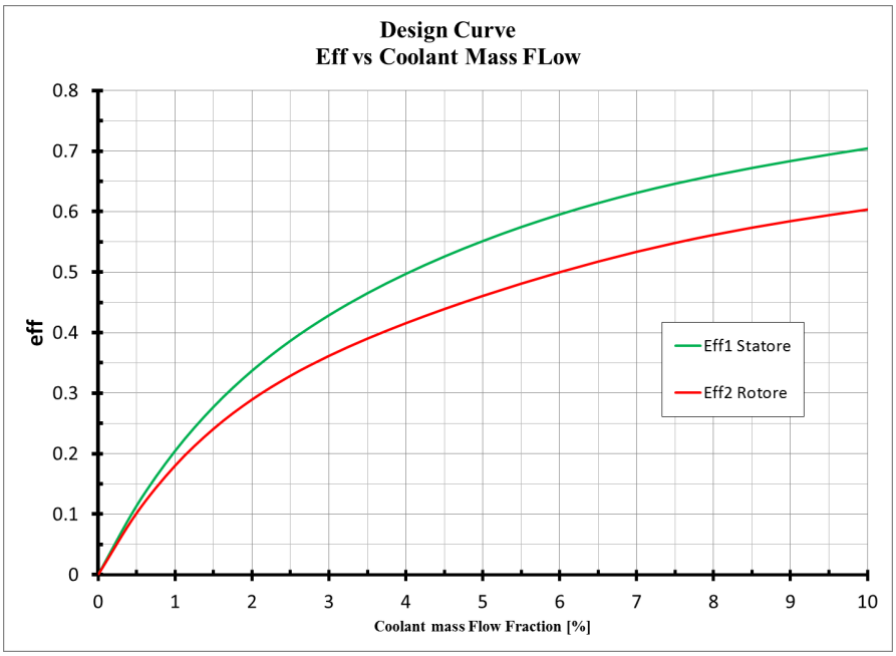

Fig. 27: RO3 Cooling Design Curve – Stator Row and Rotor Row

The curves allow to relate the cooling effectiveness to the thermal capacity ratio (or a similar quantity accounting the coolant stream).
Each curve is characteristic of a certain level of technology.

- type of cooling techniques (film cooling, transpiration, impingement, etc.)
- material properties
- blade architecture
- kind of coolant (steam, air, etc.)
- etc…

Curves similar to that of RO3 relating cooling effectiveness to thermal capacity ratio are represented in figure 28, in which the various cooling techniques represent a different curve.

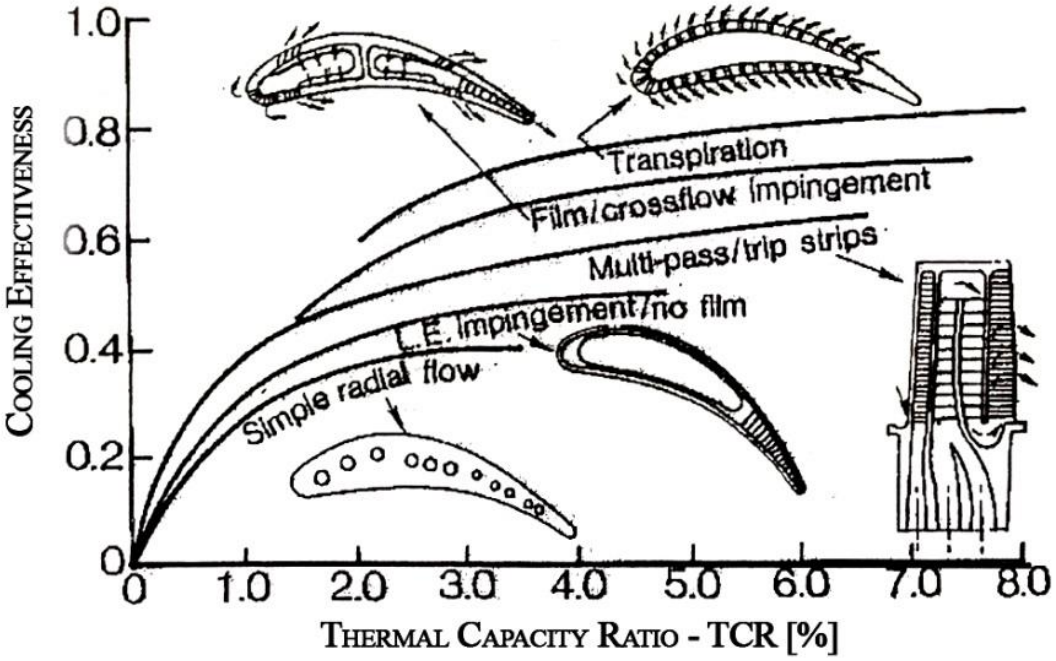

Fig. 28: Cooling Effectiveness versus Thermal Capacity Ratio

In the State of the Art of GT cooling, expression (curves) similar to that of the RO3 lumped model, relating cooling effectiveness to the coolant flows has been matched.
In figure 29, Gross Cooling Effectiveness Curves (Cooling Effectiveness defined in RO3 Model) versus heat loading parameter (accounting for coolant flow) are plotted for the various cooling techniques. In figures 30 and 31, cooling effectiveness versus coolant/gas heat flux ratio and TCR ratio are given respectively. Accordingly, trends of that curves are close to RO3 ones.

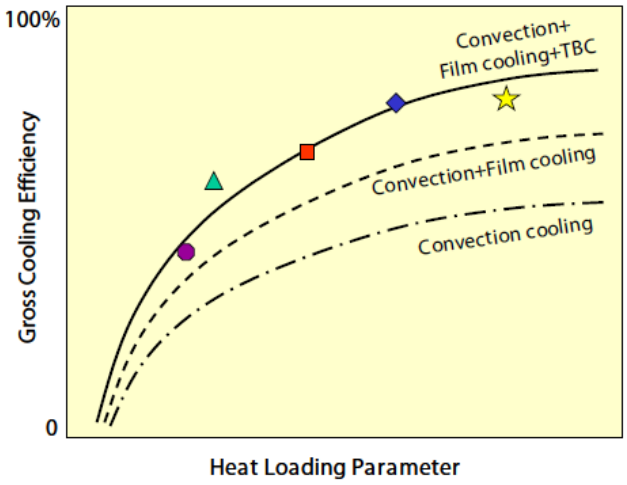

Fig. 29: SoA – Gross Cooling Effectiveness VS Heat Loading Parameter

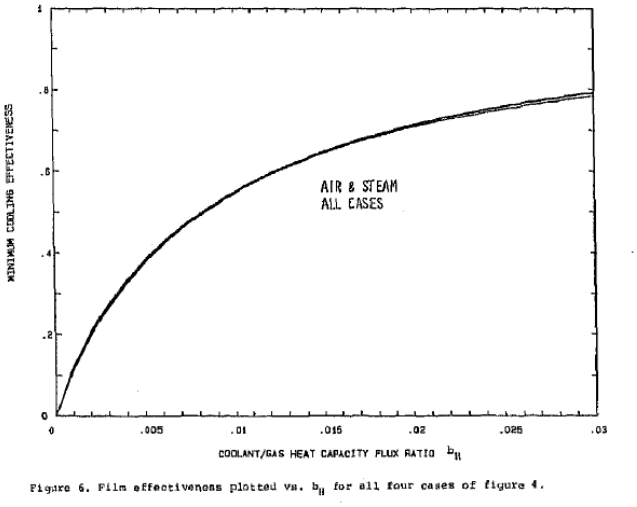

Figure 6. Film effectiveness plotted vs. b_{II} for all four cases of figure 4.

Fig. 30: SoA –Cooling Effectiveness VS Coolant/Gas Heat capacity flux ratio

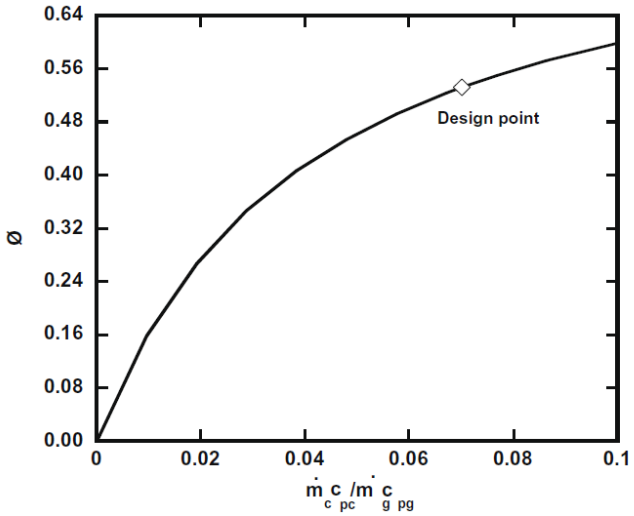

Fig. 31: SoA –Cooling Effectiveness VS TCR

7 Design Point Result

According with the lumped approach described in the paragraph 5, in RO3 University Simulator lumped cooling model the temperatures have the significant of the overall 'cooling row phenomena', thus the coolant temperature TC is not the injection temperature but the lumped reference temperature. Moreover, the coolant mass flows have the significant of the overall flow required to cool airfoil surface, disk, sealing and all the other aspects previously described.

Evaluation of coolant mass flows and of the blade wall temperature of the Lumped Model, has been performed both for the Methane fed GT and for the 33MJ/kg Syngas fed GT, being the previous one with the 1st Nozzle Vane re-staggered (opened) to maintain the same pressure ratio:

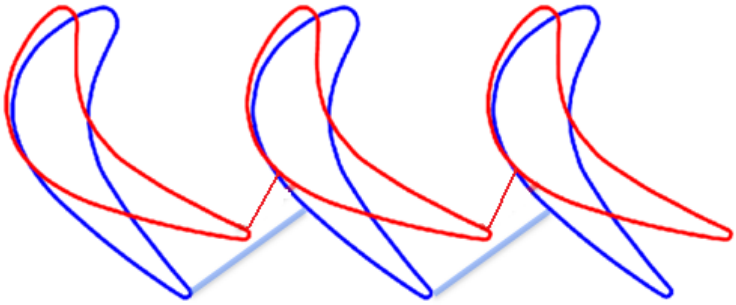

Fig. 32: 1st Nozzle Vane re-staggering – As Example

Input data for the Methane GT are given in tables 7:

Table 7: Sizing Data – Methane

Gas Expander Sizing		
Fuel	[#]	CH4
LHV	[MJ/kg]	50
VIGV	[%]	100.0
n	[rpm]	3000
pamb	[kPa]	101.3
Tamb	[°C]	15
RH	[%]	60.0
mCi	[kg/s]	685
β	[#]	18.2
TC	[°C]	500
mEi	[kg/s]	523
pex	[kPa]	104.3

In tables 8, results of Lumped Model properly adapted to the H2-IGCC context are given for Methane Fuel (50MJ/kg) fed GT

Table 8: Results of the Lumped Model for cooling requirement (Methane)

Stage	Row	mc	[kg/s]	Tb	[°C]
1	s1	ms1	44	Tbs1	895
	r1	mr1	40	Tbr1	880
2	s2	ms2	30	Tbs2	820
	r2	mr2	23	Tbr2	810
3	s3	ms3	12	Tbs3	790
	r3	mr3	15	Tbr3	760
4	s4	ms4	6	Tbs4	724
	r4	mr4	7	Tbr4	613

Input data of the sizing procedure of the cooling system are given in table 9. Results of Lumped Model properly adapted to the H2-IGCC context are given for Syngas Fuel (33MJ/kg) fed GT are presented in table 10:

Table 9: Sizing Data – 33MJ/kg Syngas

Input Data		
Fuel	[#]	Syngas
LHV	[MJ/kg]	33
VIGV	[%]	100
n	[rpm]	3000
pamb	[kPa]	101.3
Tamb	[°C]	15
RH	[%]	60.0
mCi	[kg/s]	685
β	[#]	18.2
Tc	[°C]	500.0
mEi	[kg/s]	521
pex	[kPa]	104.3

Table 10: Results of the Lumped Model for cooling requirement (33MJ/kg Syngas)

Stage	Raw	mc	[kg/s]	Tb	[°C]
1	s1	ms1	45	Ts1	895
	r1	mr1	43	Tr1	878
2	s2	ms2	31	Tbs2	821
	r2	mr2	24	Tbr2	806
3	s3	ms3	13	Tbs3	786
	r3	mr3	17	Tbr3	756
4	s4	ms4	6	Tbs4	726
	r4	mr4	7	Tbr4	614

8 Off – Design

During the Gas Turbine Operations, conditions different from the design one occur. Degradation phenomena (fouling, corrosion, erosion, etc.) influence pressure loss, heat transfer coefficients and other aspect of the high complex system of the GT cooling. Moreover, also during GT part-load behavior the various mass flows (compressor inlet, fuel, extracted flows, etc.) change owing to the different pressure differences along the machine in respect of that of the nominal point. Both the first and the second aspect are influencing continuously the GT cooling. To account these aspects, off-design curves that relate the cooling effectiveness to the Thermal Capacity Ratio have been developed.
For each Stator Vane and Rotor Blade a relation is able to describe the off-design behavior of the cooling system.

$$\eta_c = k_1(\chi) - e^{-k_2\chi}$$

$\chi = \dfrac{m_c \cdot c_{pc}}{m_g \cdot c_{pg}}$ being the Thermal Capacity Ratio TCR.

Variation on the TCR and on the capability of the system to transfer heat from the hot stream to the coolant one influences both film cooling and impingement cooling techniques. These aspects are embedded into the model by the introduction of properly coefficients (k_1, k_2). The coefficient k_1 is strictly related to the Thermal Capacity Ratio because also when TCR=0 (mc=0) some heat flows from the blade to the disks and to the casing. For this reason even if the TCR=0 the effectiveness is a little bit higher than 0.
RO3 off-design cooling model fits well with other found in the State of the Art. As an example, in figure 33 a comparison between RO3 and Kim-Ro model is presented. In relation to the TCR, the cooling effectiveness and the wall temperature for a reference blade are plotted:

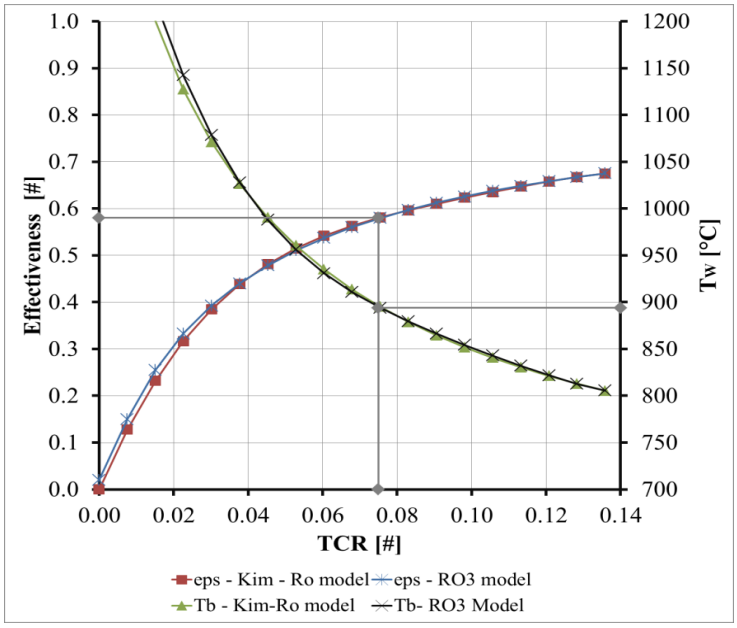

Fig. 33: Comparison between RO3 and Kim-Ro off design model

For each Stator Vane and Rotor Blade the properly cooling off-design curve has been derived taking the design (nominal) point described by an effectiveness and TCR of each row into account. In figure 35, off-design curves for each row of the 4 stage Generic 300 MW F Class GT are depicted. According to the RO3 GT cooling lumped model that considers the various heat transfer processes, off-design curves have been presented also for the uncooled stages (blade not internally cooled by the coolant flows) in which anyway some heat is conducted by the blade to the disk and also drained to the other components. This heat should be removed to maintain the hot components temperature under the maximum allowable temperature. In figure 34 a sketch of a uncooled blade is depicted.

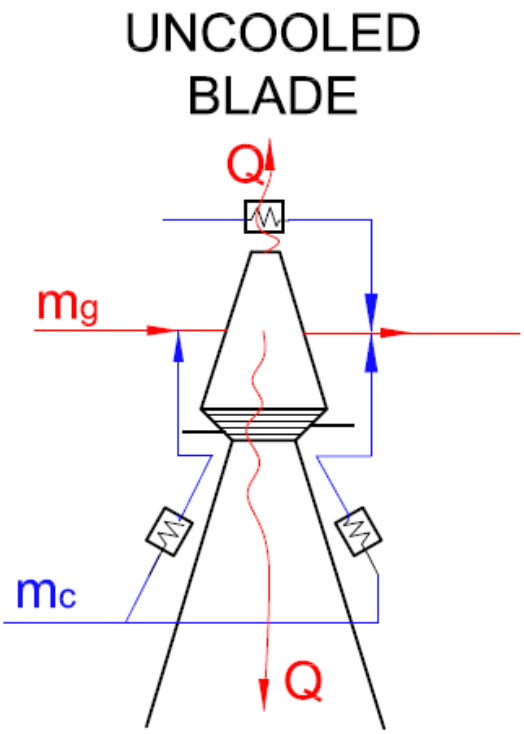

Fig. 34: Uncooled Blade Row Scheme – As Example

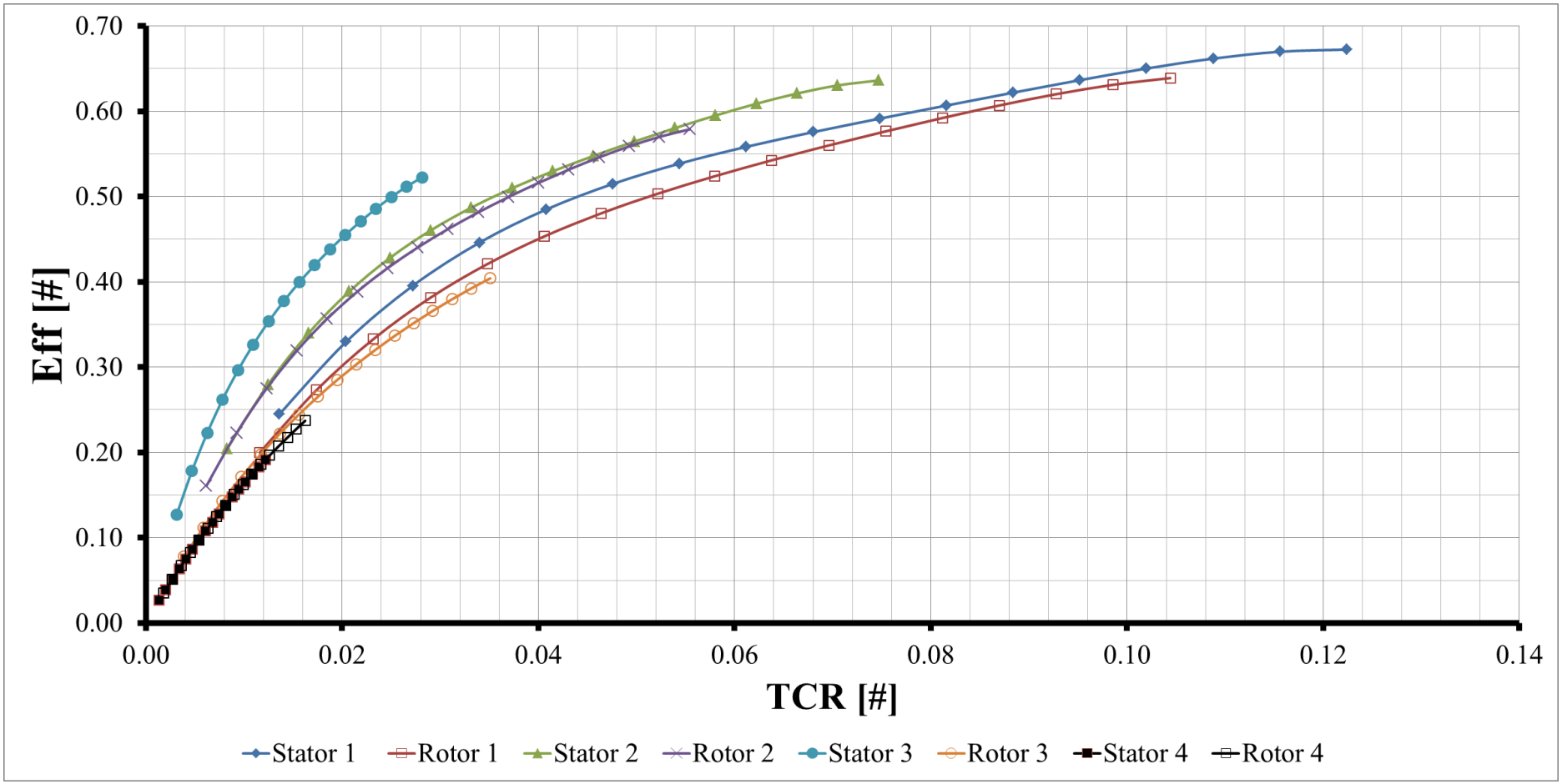

Fig. 35: Off-Design cooling effectiveness VS TCR

Reference

[1] Ainely D. G., Internal Air-Cooling for Turbine Blades – A General Design Survey, Minestry of Supply, Aeronautical Research Council Reports and Memoranda, London 1957

[2] Albeirutty M. H, Alghamdi A. S., Najjar Y. S., "Heat transfer analysis for a multistage gas turbine using different blade-cooling schemes, ELSEVIER Applied Thermal Engineering 24 (2004), 563-577

[3] Boyce M.P., Gas Turbine Engineering Handbook 2nd edition, Gulf Publishing Company, 2002

[4] Carcasci C., Facchini B., A numerical procedure to design internal cooling of a gas turbine stator blades, ELSEVIER Revue Générale de Thermique 35 (1996), 257-268

[5] Cerri, G., Marra, C., Sorrenti, A., Spinosa, S., 1990a, "Iniezione di vapore nelle turbine a gas e raffreddamento delle palette: considerazioni teoriche," *IV Convegno Nazionale Gruppi Combinati Prospettive Tecniche ed Economiche*, Florence, Italy, May 31

[6] Cerri, G., Marra, C., Sorrenti, A., Spinosa, S., 1990b, "Iniezione di vapore nelle turbine a gas e raffreddamento delle palette: analisi di un'applicazione," *IV Convegno Nazionale Gruppi Combinati Prospettive Tecniche ed Economiche*, Florence, Italy, May 31

[7] Cohen H., Rogers G.F.C., Saravanamuttoo H.I.H., Gas Turbine Theroy 3rd edition, Longman Scientific & Technical, 1987

[8] Facchini B., Ferrara G., Innocenti L., ELSEVIER International Journal of Thermal Science 39 (2000), 74-84

[9] Han J.C., Dutta S., Ekkad S.V., Gas Turbine Heat Transfer and Cooling Technologiy, Taylor and Franis, 2000

[10] Logan E., Roy R., Handbook of Turbomachinery 2nd edition Revised and Expanded, Marcel Dekker, 2003

[11] Sanjay, Singh O., Prasad B.N., Comparative performance analysis of cogeneration gas turbine cycle for different blade cooling means, ELSEVIER International Journal of Thermal Science 48 (2009), 1432-1440.

[12] Sanjay K., Singh O., Thermodynamic Evaluation of different gas turbine blade cooling techniques, Thermal Issues in Emerging Technologies, ThETA 2, Cairo, Egypet, Dec 17-20th 2008

[13] *Jonsson M., Bolland O., Bucker D., Rost M. (Siemens), 2005, 'Gas Turbine Cooling Model for Evaluation of Novel Cycles'. Proceedings of ECOS 2005, Trondheim, Norway, June 20-22, 2005*